Precyzyjne testy Modelu Standardowego i jego rozszerzeń

Janusz Gluza, Uniwersytet Śląski w Katowicach

XLIX Zjazd Fizyków i Fizyczek Polskich

9.09.2025, Katowice

'Precise measurements of known particles and interactions are just as important as finding new particles'

– Fabiola Gianotti

MS potwierdzony, dwa punkty widzenia

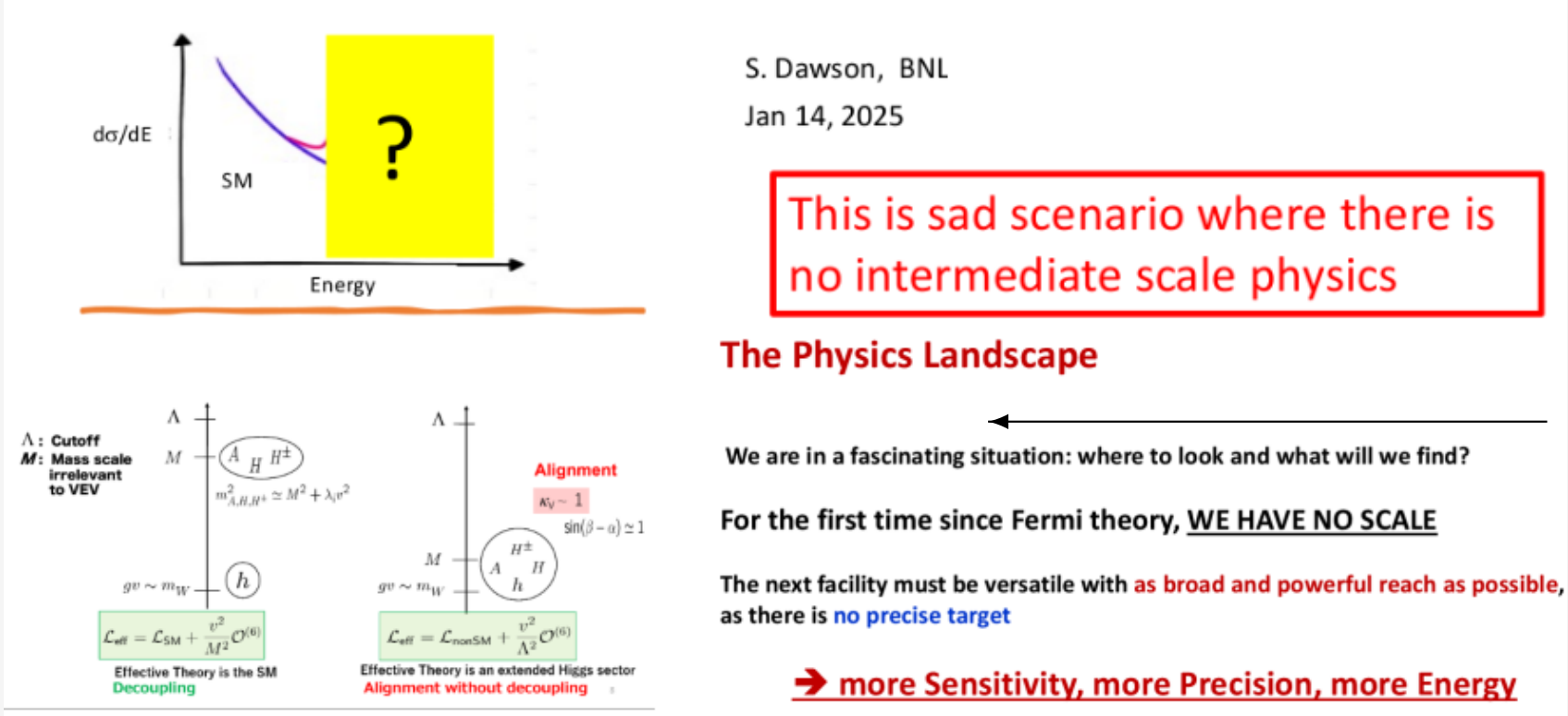

plot by Kanemura

S. Dawson, BNL

Jan 14, 2025

This is sad scenario where there is no intermediate scale physics

The Physics Landscape

We are in a fascinating situation: where to look and what will we find?

For the first time since Fermi theory, WE HAVE NO SCALE

The next facility must be versatile with as broad and powerful reach as possible, as there is no precise target

➔ more Sensitivity, more Precision, more Energy

A. Blondel, Epiphany 2021

Precyzyjne przewidywania SM stanowia podstawe do konfrontacji z każdym, szczególnie małym niestandardowym efektem, który poszukujemy!

PRECYZJA

Model Standardowy

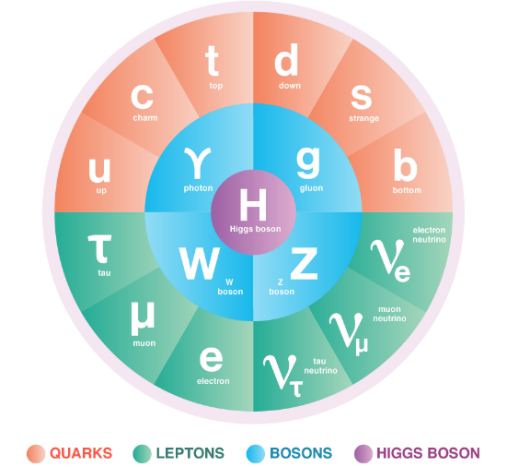

"Whoever has only a hammer will see nothing but nails."

Serial dokumentalny BBC, Precision: The Measure of All Things

Stałe fizyczne, PDG2025 (Particle Data Group)

Quantity	Symbol, equation	Value	Uncertainty (ppb)
speed of light in vacuum	c	299 792 458 m s^{-1}	exact
Planck constant	h	$6.626\ 070\ 15\times10^{-34}$ J s (or J/Hz) §	exact
Planck constant, reduced	$\hbar \equiv h/2\pi$	$1.054\ 571\ 817\ldots\times10^{-34}$ J s	exact*
		$= 6.582\ 119\ 569\ldots\times10^{-22}$ MeV s	exact*
electron charge magnitude	e	$1.602\ 176\ 634\times10^{-19}$ C	exact
conversion constant	$\hbar c$	197.326 980 4... MeV fm	exact*
conversion constant	$(\hbar c)^2$	0.389 379 372 1... GeV^2 mbarn	exact*
electron mass	m_e	0.510 998 950 00(15) MeV/c^2 = $9.109\ 383\ 7015(28)\times10^{-31}$ kg	0.30
proton mass	m_p	938.272 088 16(29) MeV/c^2 = $1.672\ 621\ 923\ 69(51)\times10^{-27}$ kg	0.31
		= 1.007 276 466 621(53) u = 1836.152 673 43(11) m_e	0.053, 0.060
neutron mass	m_n	939.565 420 52(54) MeV/c^2 = 1.008 664 915 95(49) u	0.57, 0.48
deuteron mass	m_d	1875.612 942 57(57) MeV/c^2	0.30
unified atomic mass unit**	u = (mass ^{12}C atom)/12	931.494 102 42(28) MeV/c^2 = $1.660\ 539\ 066\ 60(50)\times10^{-27}$ kg	0.30
fine-structure constant	$\alpha = e^2/4\pi\epsilon_0\hbar c$	$7.297\ 352\ 5693(11)\times10^{-3} = 1/137.035\ 999\ 084(21)$ †	0.15
classical electron radius	$r_e = e^2/4\pi\epsilon_0 m_e c^2$	$2.817\ 940\ 3262(13)\times10^{-15}$ m	0.45
(e^- Compton wavelength)/2π	$\lambda\!\!\!^{-}_e = \hbar/m_e c = r_e\alpha^{-1}$	$3.861\ 592\ 6796(12)\times10^{-13}$ m	0.30
Bohr radius ($m_{\rm nucleus} = \infty$)	$a_\infty = 4\pi\epsilon_0\hbar^2/m_e e^2 = r_e\alpha^{-2}$	$0.529\ 177\ 210\ 903(80)\times10^{-10}$ m	0.15
wavelength of 1 eV/c particle	hc/(1 eV)	$1.239\ 841\ 984\ldots\times10^{-6}$ m	exact*
Rydberg energy	$hcR_\infty = m_e e^4/2(4\pi\epsilon_0)^2\hbar^2 = m_e c^2\alpha^2/2$	13.605 693 122 994(26) eV	1.9×10^{-3}
Thomson cross section	$\sigma_T = 8\pi r_e^2/3$	0.665 245 873 21(60) barn	0.91

[a]Updated values reflecting the "2022 CODATA recommended values", released online in May 2024, will be incorporated in future editions of the *Review*.
§CODATA recommends that the unit be J/Hz to stress that in $h = E/\nu$ the frequency ν is in cycles/sec (Hz), not radians/sec.
*These are calculated from exact values and are exact to the number of places given (*i.e.* no rounding).
**The molar mass of ^{12}C is 11.999 999 9958(36) g.
†CODATA recommended value at $Q^2 = 0$. At $Q^2 \approx m_W^2$ the value is $\sim 1/128$. A world average of the latest data yields $\alpha^{-1} = 137.035999178(8)$. ‡‡
‡Absolute laboratory measurements of G_N have been made only on scales of about 1 cm to 1 m.

https://pdg.lbl.gov/2025/reviews/rpp2024-rev-phys-constants.pdf

Postępy Fizyki, https://jgluza.us.edu.pl/kg.pdf

Ku nowej definicji kilograma

Janusz Gluza, Agnieszka Grzanka, Agnieszka Pleban

Instytut Fizyki, Uniwersytet Śląski, Katowice

Towards a redefinition of the kilogram

Abstract: Recent attempts at a redefinition of the kilogram are shortly described.

1. Wstęp

Wszystkie podstawowe jednostki miar układu SI poza kilogramem zdefiniowane są w sposób uniwersalny, natomiast odtworzenie wzorca masy wymaga bezpośredniego porównania danej próbki z oryginałem lub jedną z jego oficjalnych kopii. W artykule opisujemy próby zdefiniowania także jednostki masy w sposób fundamentalny, za pomocą precyzyjnych doświadczeń, opartych m.in. na efektach kwantowych. Fizycy pracujący nad tym zagadnieniem mają nadzieję, że ich eksperymenty będzie można w przyszłości powielać, tak by odtworzenie kilograma w przeciętnym laboratorium fizycznym nie stanowiło problemu. Czy zmiana definicji kilograma nastąpi już w roku 2007, jak sugerują w swoich pracach niektórzy autorzy? Niekoniecznie, ale chyba nieuchronnie nadchodzi czas takiej zmiany.

2. Trochę historii i stan obecny

Król Ludwik XVI w 1790 r. zobowiązał francuskich uczonych do stworzenia spójnego systemu jednostek wag i miar – systemu metrycznego. Już 19 marca 1791 r. Francuska Akademia Nauk przyjęła definicję jednostki masy opartej na ściśle określonej objętości (1 dm^3, czyli praktycznie jednego litra) destylowanej wody w temperaturze, w której ma ona największą gęstość, tj. ok. 4 °C. Za datę powstania międzynarodowego układu miar SI (Système International d'Unités) opartego na systemie dziesiętnym należy jednak uznać 22 czerwca 1799 r., kiedy to w Archives de la République w Paryżu zdeponowano dwa platynowe wzorce: metra oraz kilograma (tzw. Kilogramme des Archives). Ważnym krokiem w historii SI było utworzenie w 1875 r. Międzynarodowego Biura Miar i Wag (BIPM, Bureau International des Poids et Mesures) w Sèvres pod Paryżem.

Kilogramme des Archives miał kształt walca i wyko-

ności na czynniki zewnętrzne. Dlatego przyjęto radę francuskiej sekcji międzynarodowej komisji metra CIM (Commission Internationale du Mètre), aby użyć wytworzonego przez francuskiego chemika Henriego Sainte-Claire Deville'a i jego ucznia Henriego Debray stopu platyny z irydem. Stop ten był zdecydowanie twardszy od czystej platyny i miał dodatkowe pożądane właściwości (większą odporność na korozję, większą gęstość, dobre przewodnictwo ciepła i prądu, mniejszą wrażliwość na pole magnetyczne). Masową produkcją stopu zajęła się firma Johnson Matthey (JM).

Pierwsze trzy prototypy kilograma zostały wykonane właśnie w fabryce JM i nadano im nazwy KI, KII, KIII. Prototypy te porównano w Obserwatorium Paryskim z Kilogramme des Archives i ostatecznie jako międzynarodowy wzorzec kilograma przyjęto prototyp KIII. Wzorzec ten został usankcjonowany uchwałą I Generalnej Konferencji Miar w 1889 r., a za jego symbol przyjęto literę $\mathfrak{K}$ (tzw. Grand K). Jest to walec o średnicy i wysokości po 39 milimetrów (rys. 1), wykonany w 90% z platyny; resztę stanowi iryd.

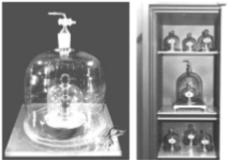

Największa rewolucja w pomiarach od czasu rewolucji francuskiej:

nowa definicja jednostki masy

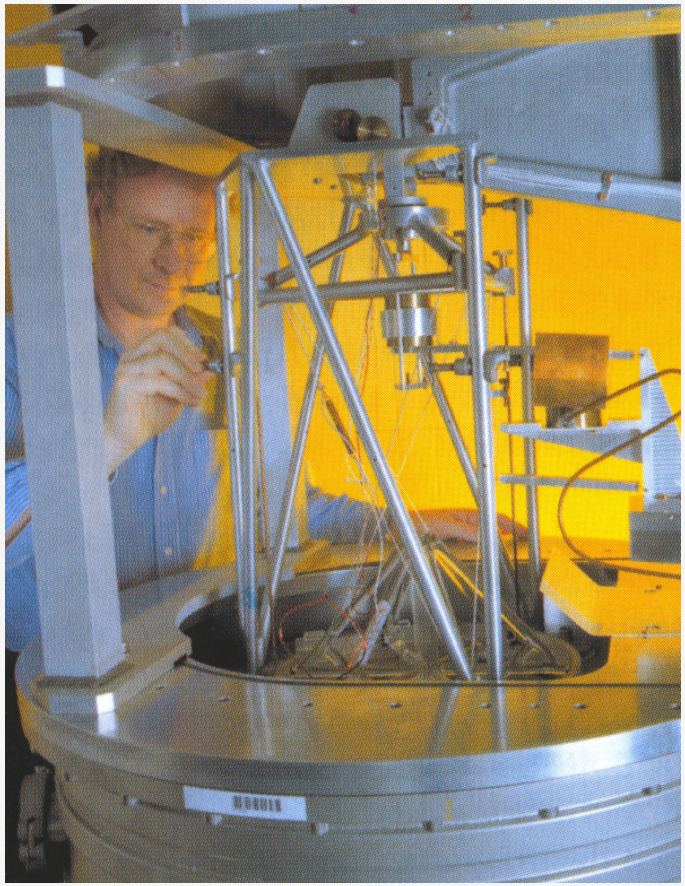

Definicje jednostki masy

- Nowa definicja, 2019:
  "Kilogram, oznaczenie kg, jest to jednostka masy w układzie SI. Jest ona zdefiniowana poprzez przyjęcie ustalonej wartości liczbowej stałej Plancka h, wynoszącej $6.62607015 \cdot 10^{-34}$, wyrażonej w jednostce $J \cdot s$, która jest równa $kg \cdot m^2 \cdot s^{-1}$, przy czym metr i sekunda zdefiniowane są za pomocą c i f_{Cs}."
- Czyli mamy związek:

$$kg \leftrightarrow h, m(c), s(f_{Cs})$$

.

Balans Watta: idea (Postępy fizyki, 2007)

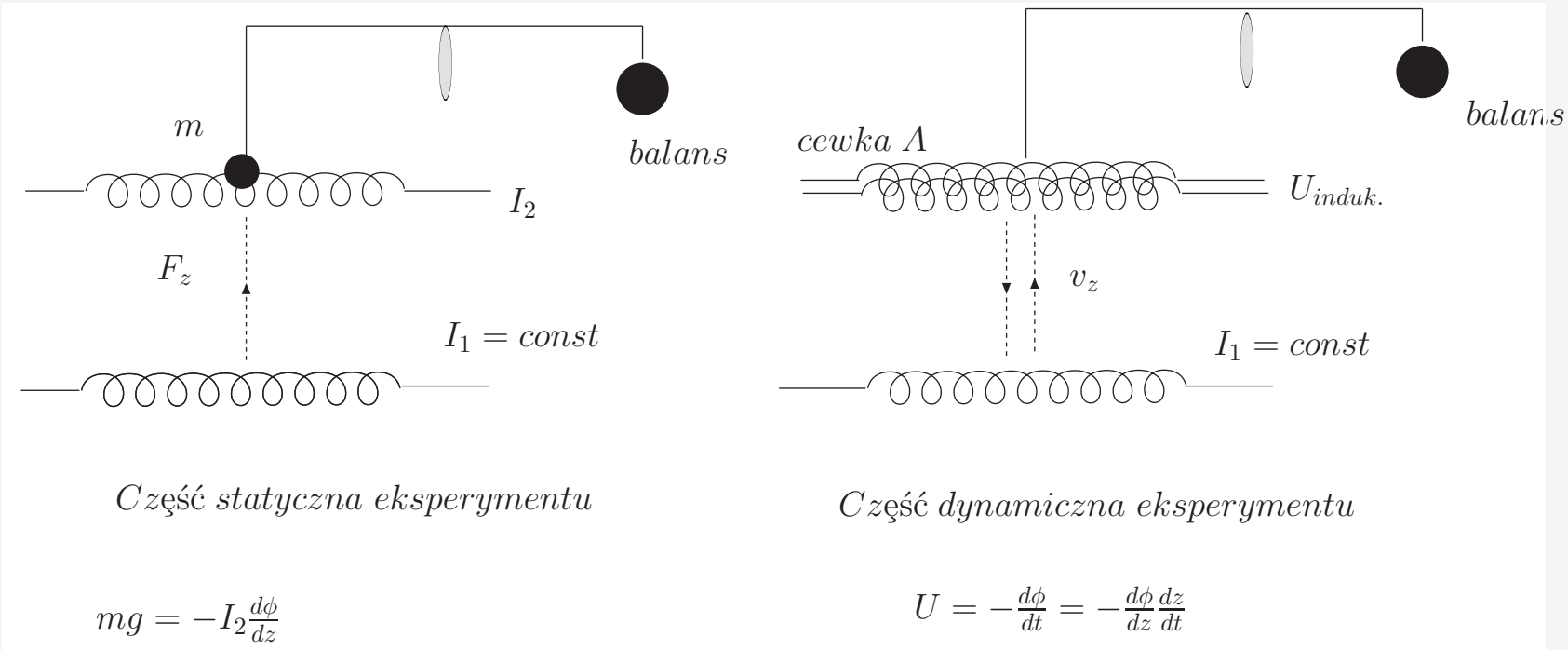

Część statyczna eksperymentu

$mg = -I_2 \frac{d\phi}{dz}$

Część dynamiczna eksperymentu

$U = -\frac{d\phi}{dt} = -\frac{d\phi}{dz}\frac{dz}{dt}$

Balans równoważy cewkę A

$$mgv = U_{induk.} I_2$$

U, I - kwantowe efekty (prąd tunelowy - stała Josphsona $\propto e/h$, oporność - stała von Klitzinga $\propto h/e$.

How We're Redefining the kg

Filmik z NIST. *https://www.youtube.com/watch?v=Oo0jm1PPRuo*

specjalny budynek ....

Układ SI (od 1790) definiuje 7 podstawowych jednostek fizycznych

Wielkość	Jednostka	względna dokładność
Długość	m	1×10^{-12}
Masa	kg	1×10^{-8}
Czas	s	$\mathbf{3 \times 10^{-15}}$
Prąd	A	4×10^{-8}
Temperatura	K	3×10^{-7}
Świetlność	kandela	1×10^{-4}
Miara substancji	mol	8×10^{-8}

Dokładność: błąd sekundy raz na 20 mln lat - ważne np. w GPS, komórki, internet.

https://www.nature.com/articles/s41586-021-03253-4 - "Frequency ratio measurements at 18-digit accuracy using an optical clock network" - Nature, 2021

Stała struktury subtelnej - α_{QED} - nowy wynik (2020)

REPORT

Measurement of the fine-structure constant as a test of the Standard Model

Richard H. Parker[1,*], Chenghui Yu[1,*], Weicheng Zhong[1], Brian Estey[1], Holger Müller[1,2,†]
+ See all authors and affiliations

Science 13 Apr 2018:
Vol. 360, Issue 6385, pp. 191-195
DOI: 10.1126/science.aap7706

Article | Published: 02 December 2020

Determination of the fine-structure constant with an accuracy of 81 parts per trillion

Léo Morel, Zhibin Yao, Pierre Cladé & Saïda Guellati-Khélifa

Nature **588**, 61–65(2020) | Cite this article

$\alpha^{-1}(Cs)$= 137.035 999 046(27)

$\alpha^{-1}(Rb)$= 137.035 999 206(11)

$\alpha^{-1}(a_e)$= 137.035 999 139(31)

Uwaga: (i) nowy wynik już odchylenie od SM w kierunku jak dla $(g-2)_\mu$, (ii) duża rozbieżność z Cs ($\sim 5.4\sigma$).

Guellati-Khélifa poprawiała eksperyment 22 lata[1]
https://www.nature.com/articles/s41586-020-2964-7 [02 December 2020]

$$R_\infty = \frac{\alpha^2 m_e c}{4\pi\hbar} \longrightarrow \alpha^2 = \frac{R_\infty}{c} \times \frac{h}{m_e} \longrightarrow \frac{h}{m_e} = \frac{u}{m_e}\frac{M_X}{u}\frac{h}{M_X}$$

[1] Jaki najdłuższy eksperyment w historii?

Fizyka wysokich energii zmienia obraz, $\alpha_{QED}(s)$, polaryzacja próżni

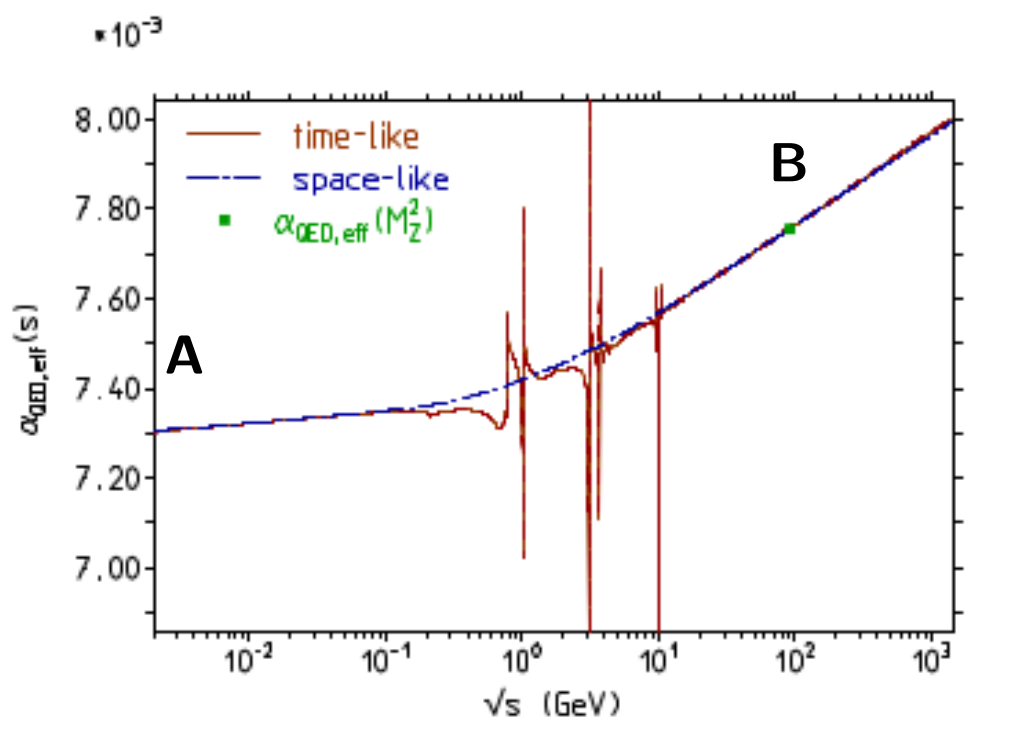

A: $\alpha_{QED}(0) \simeq 1/137$

B: $\alpha_{QED}(M_Z^2) \simeq 1/128$

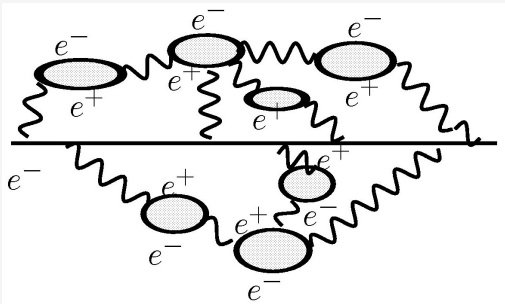

F. Jegerlehner, http://dx.doi.org/10.23731/CYRM-2020-003.9

Efektywna $\alpha(s)$ w funkcji fotonowej polaryzacji próżni $\Delta\alpha(s)$

$$\alpha(s) = \frac{\alpha}{1-\Delta\alpha(s)}\Delta\alpha(s) = \Delta\alpha_{\rm lep}(s) + \Delta\alpha_{had} + \Delta\alpha_{\rm top}(s)\,.$$

Fizyka cząstek elementarnych

gravitational constant‡	G_N	$6.674\ 30(15)\times10^{-11}$ m^3 kg^{-1} s^{-2}	2.2×10^4
		$= 6.708\ 83(15)\times10^{-39}$ $\hbar c$ (GeV/c^2)$^{-2}$	2.2×10^4
standard gravitational accel.	g_N	9.806 65 m s^{-2}	exact
Avogadro constant	N_A	$6.022\ 140\ 76\times10^{23}$ mol^{-1}	exact
Boltzmann constant	k	$1.380\ 649\times10^{-23}$ J K^{-1}	exact
		$= 8.617\ 333\ 262\ldots\times10^{-5}$ eV K^{-1}	exact*
molar volume, ideal gas at STP	$N_A k$ (273.15 K)/(101 325 Pa)	$22.413\ 969\ 54\ldots\times10^{-3}$ m^3 mol^{-1}	exact*
Wien displacement law constant	$b = \lambda_{\max} T$	$2.897\ 771\ 955\ldots\times10^{-3}$ m K	exact*
Stefan-Boltzmann constant	$\sigma = \pi^2 k^4/60\hbar^3 c^2$	$5.670\ 374\ 419\ldots\times10^{-8}$ W m^{-2} K^{-4}	exact*
Fermi coupling constant‡‡	$G_F/(\hbar c)^3$	$1.166\ 378\ 8(6)\times10^{-5}$ GeV^{-2}	510
weak-mixing angle‡‡	$\sin^2\widehat{\theta}(M_Z)$ $(\overline{\rm MS})$	0.231 29(4)††	1.7×10^5
$W^\pm$ boson mass	m_W	80.3692(133) GeV/c^2¶	1.7×10^5
Z^0 boson mass	m_Z	91.1880(20) GeV/c^2‖	2.2×10^4
strong coupling constant	$\alpha_s(m_Z)$	0.1180(9)	7.6×10^6

$\pi = 3.141\ 592\ 653\ 589\ 793\ 238\ldots$		$e = 2.718\ 281\ 828\ 459\ 045\ 235\ldots$	$\gamma = 0.577\ 215\ 664\ 901\ 532\ 860\ldots$
1 in $\equiv$ 0.0254 m	1 G $\equiv 10^{-4}$ T	1 eV = $1.602\ 176\ 634\times10^{-19}$ J (exact)	kT at 300 K = $[38.681\ 727\ 0718\ldots]^{-1}$eV (exact*)
1 Å $\equiv$ 0.1 nm	1 dyne $\equiv 10^{-5}$ N	$(1\text{ kg})c^2 = 5.609\ 588\ 603\ldots\times10^{35}$ eV(exact*)	0 °C $\equiv$ 273.15K
1 barn $\equiv 10^{-28}$ m^2	1 erg $\equiv 10^{-7}$ J	1 C = $2.997\ 924\ 58\times10^9$ esu	1 atmosphere $\equiv$ 760 Torr $\equiv$ 101 325Pa

[a]Updated values reflecting the "2022 CODATA recommended values", released online in May 2024, will be incorporated in future editions of the *Review*.
§CODATA recommends that the unit be J/Hz to stress that in $h = E/\nu$ the frequency ν is in cycles/sec (Hz), not radians/sec.
*These are calculated from exact values and are exact to the number of places given (*i.e.* no rounding).
**The molar mass of ^{12}C is 11.999 999 9958(36) g.
†CODATA recommended value at $Q^2 = 0$. At $Q^2 \approx m_W^2$ the value is $\sim 1/128$. A world average of the latest data yields $\alpha^{-1} = 137.035999178(8)$. ‡‡
‡Absolute laboratory measurements of G_N have been made only on scales of about 1 cm to 1 m.

https://pdg.lbl.gov/2025/reviews/rpp2024-rev-phys-constants.pdf

Precyzja, fizyka cząstek

- (i) odkrycie mionu, J/Ψ
  (ii) $(g-2)_e$, $(g-2)_\mu$ EKSPERYMENT $\rightarrow$ TEORIA
  (iii) V-A, parzystość;

- (i) $\tau^{\pm}$ (tau lepton);
  (ii) Tevatron - odkrycie kwarku top; TEORIA $\rightarrow$ EKSPERYMENT
  (iii) H^0 (skalarny boson (Higgs-Englert...)

  ważne SM poprawki kwantowe! LEP, SLAC, LHC
  M. Veltman (1977) ρ-parametr $\sim m_t^2, \ln(m_H^2)$;
  $\longrightarrow$ Acta Physica Polonica B

BOOK
Special volume of Acta Physica Polonica B commemorating Martinus Veltman
by **Jadach, Stanisław; Jeżabek, Marek; Praszałowicz, Michał**

Published by **Acta Physica Polonica 2021**

This memorial volume of Acta Physica Polonica B is a special tribute to the Nobel Laureate Martinus Veltman. Professor Veltman was a member of the APPB International Editorial Council, lecturer at the Cracow School of Theoretical Physics in 1977 and 1994, and the author of two the most cited articles ever published in our journal: «Second Threshold in Weak Interactions» [Acta Phys. Pol. B 8, 475 (1977)] and «The Infrared–Ultraviolet Connection» [Acta Phys. Pol. B 12, 437 (1981)].

- Neutrina (masy, mieszania, CP faza(y);
  Super-K, Hyper-K, T2K, NOvA, Antares, KM3NeT, Juno, Dune,
  SNO+, Daya Bay, Double Chooz, RENO, ...

Przyszłe zderzacze; TEORIA $\leftrightarrow$ EKSPERYMENT

Z.Ligeti

Aside: factor-of-2 improvements can matter!

Search for $K_L \to \pi\pi$

ANNALS OF PHYSICS: 5, 156–181 (1958)

Long-lived Neutral K Mesons*

M. BARDON, K. LANDE, AND L. M. LEDERMAN

Columbia University, New York, New York, and Brookhaven National Laboratories, Upton, New York

AND

WILLIAM CHINOWSKY

Brookhaven National Laboratories, Upton, New York

set an upper limit <0.6% on the reactions

< 0.6%

$$K_2^0 \to \begin{cases} \mu^{\pm} + e^{\mp} \\ e^+ + e^- \\ \mu^+ + \mu^- \end{cases}$$

and on $K_2^0 \to \pi^+ + \pi^-$.

VOLUME 6, NUMBER 10 PHYSICAL REVIEW LETTERS MAY 15, 1961

DECAY PROPERTIES OF K_2^0 MESONS*

D. Neagu, E. O. Okonov, N. I. Petrov, A. M. Rosanova, and V. A. Rusakov
Joint Institute of Nuclear Research, Moscow, U.S.S.R.
(Received April 20, 1961)

Combining our data with those obtained in reference 7, we set an upper limit of 0.3% for the relative probability of the decay $K_2^0 \to \pi^- + \pi^+$. Our

< 0.3%

"At that stage the search was terminated by administration of the Lab."

[Okun, hep-ph/0112031]

VOLUME 13, NUMBER 4 PHYSICAL REVIEW LETTERS 27 JULY 1964

EVIDENCE FOR THE 2π DECAY OF THE K_2^0 MESON*†

J. H. Christenson, J. W. Cronin,‡ V. L. Fitch,‡ and R. Turlay§
Princeton University, Princeton, New Jersey
(Received 10 July 1964)

= 0.2 ± 0.04 %

We would conclude therefore that K_2^0 decays to two pions with a branching ratio $R = (K_2 \to \pi^+ + \pi^-)/(K_2^0 \to \text{all charged modes}) = (2.0 \pm 0.4) \times 10^{-3}$ where the error is the standard deviation. As empha-

Precyzyjne obliczenia, Katowice

particles.us.edu.pl/czastki.us.edu.pl

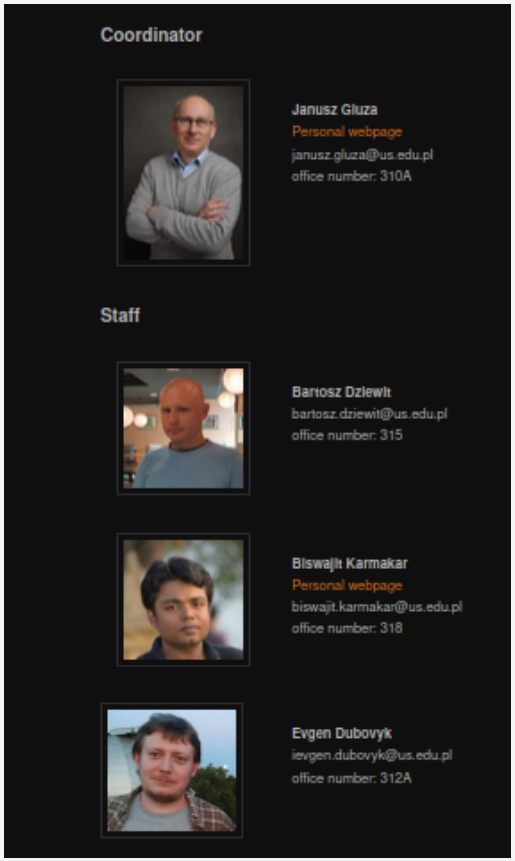

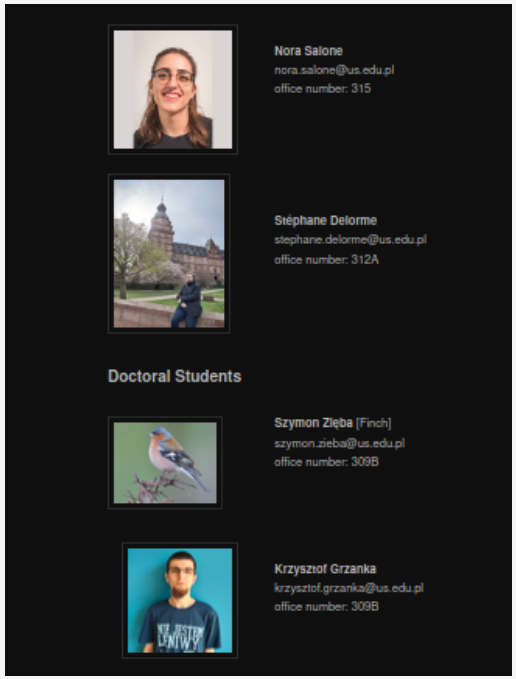

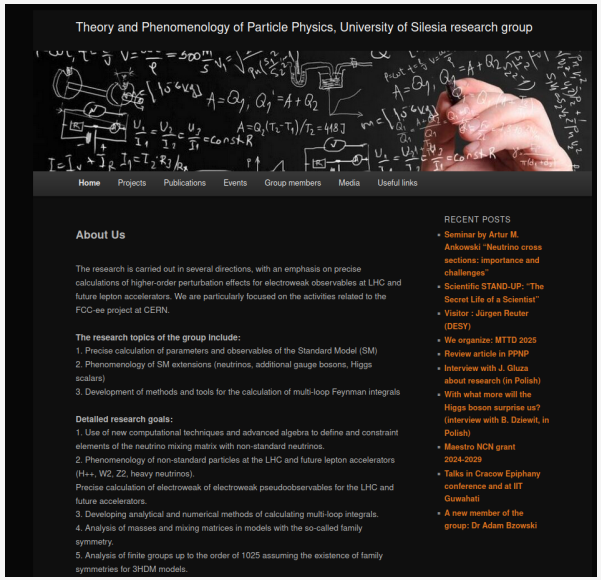

Generatory MC, teoria (rezonans bozonu Z), perturbacyjne poprawki kwantowe

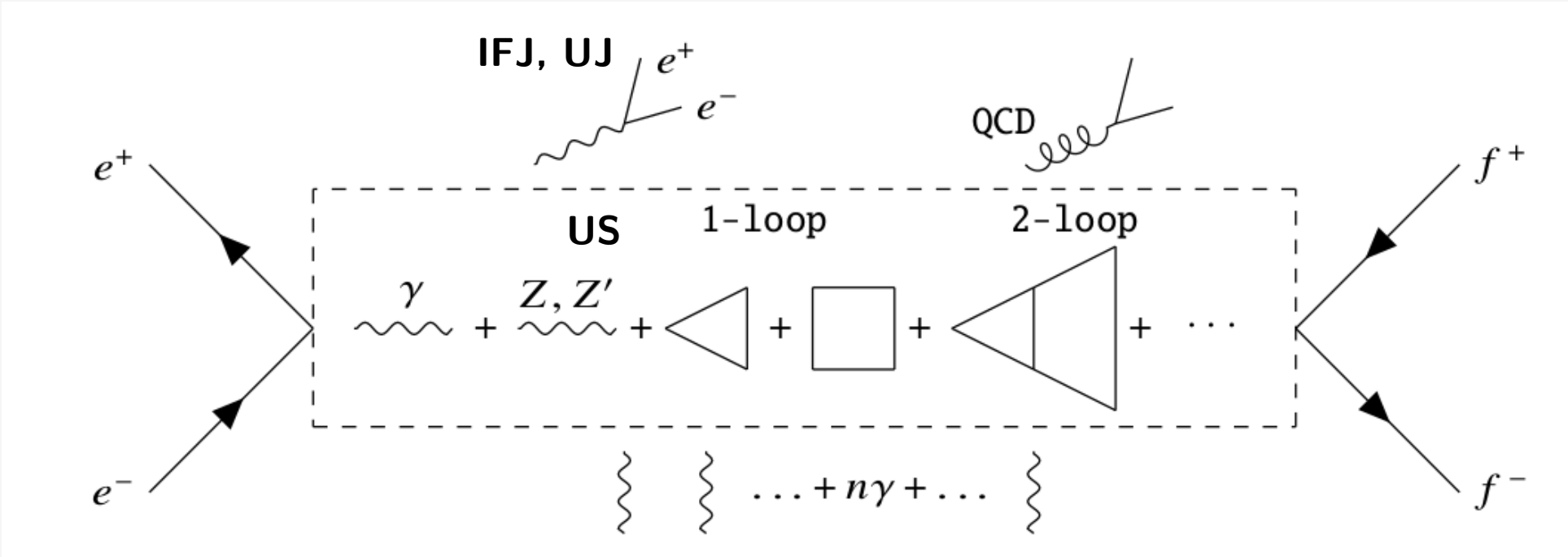

Współpraca Kraków - Katowice, 2024-2029, grant NCN

Future Circular Collider – A key to new physics

The Future Circular Collider (FCC) study is an international collaboration aimed at designing the particle accelerator that will replace the LCH once it has completed its operational lifetime. The FCC will expand the current energy and luminosity frontiers in order to help answer the most fundamental questions in science: What is dark matter? Are there extra dimensions in the universe? Are there other forces in nature?

The FCC collaboration, hosted by CERN, is open to universities, research institutes and high-tech companies. A conceptual design will be delivered before the end of 2018, in time for the next update of the European Strategy for Particle Physics.

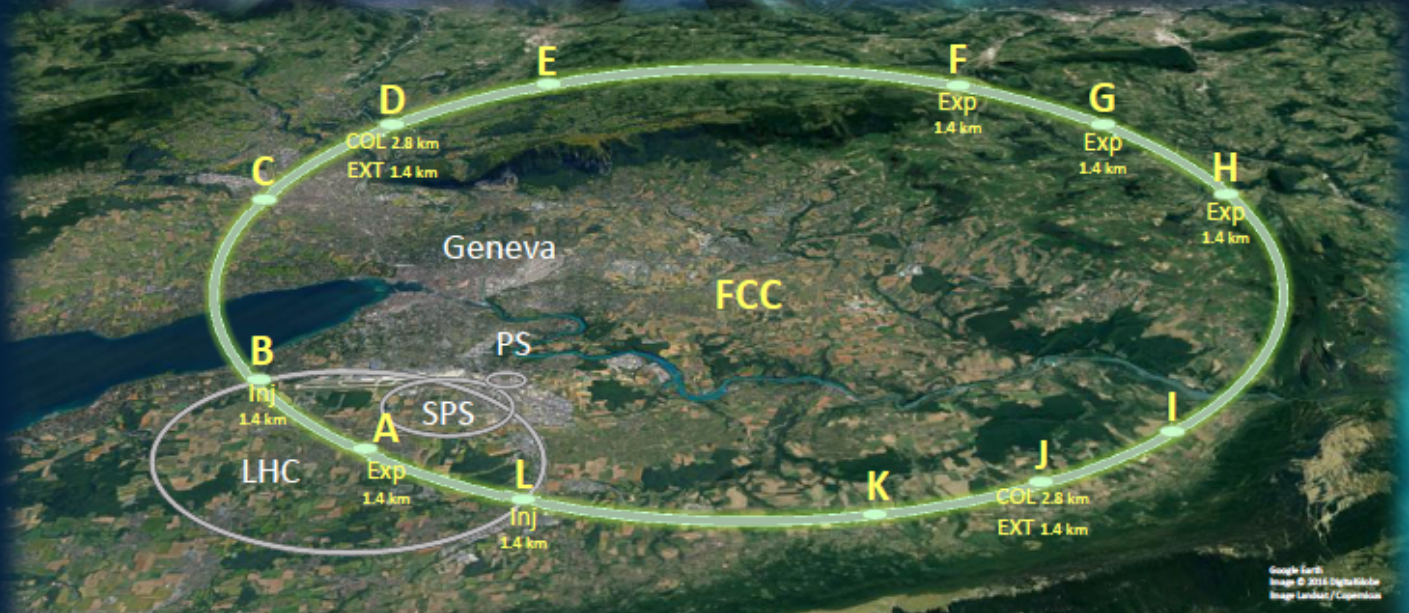

FCC-hh – A discovery machine

The 100 TeV proton-proton collider (FHC-hh) will have an energy seven times higher than the LHC. Such a collider will give access to the smallest scales and the most energetic phenomena in nature.

New fundamental forces and particles can be discovered, extending the reach for searching dark matter particles, supersymmetric partners of quarks and gluons, and possible substructure inside quarks.

Billions of Higgs bosons and trillions of top quarks will be produced, creating new opportunities for the study of rare decays, flavor physics, and the mechanism of electroweak symmetry breaking.

The FCC-hh collider provides also the opportunity to push the exploration of the collective structure of matter at the most extreme density and temperature conditions to new frontiers through the study of heavy-ion collisions.

FCC-ee – A machine for precision

The second scenario of the FCC design study (FCC-ee) is a high-luminosity, high-precision electron-positron collider with center-of-mass collision energies between 90 and 350 GeV. Located in the same 100 km long tunnel as the FCC-hh it is considered a potential intermediate step towards the realization of the hadron facility, and complementary to it.

Clean experimental conditions give electron-positron colliders the capability to measure known particles with the highest precision.

FCC-ee would measure the properties of the Z, W, Higgs and top particles with unequalled accuracy, offering the potential for discovering dark matter or heavy neutrinos. The FCC-ee could enable profound investigations of electroweak symmetry breaking and open a broad indirect search for new physics over several orders of magnitude in energy.

FCC-he – New opportunities

With the huge energy provided by the 50 TeV proton beam and the potential availability of an electron beam with energies of the order of 60 GeV, new horizons open up for the physics of deep inelastic electron-proton scattering.

The FCC-he collider would be both a high-precision Higgs factory and a powerful microscope to discover new particles. It would be the most accurate tool for studying quark-gluon interactions, possible substructure of matter and unprecedented measurements of strong and electroweak interaction phenomena. The hadron-electron collider is a unique complement to the exploration of nature at high energies within the FCC complex.

The FCC study explores three different scenarios: a hadron-had collider (FCC-hh), an electron-positron collider (FCC-ee), an hadron-lepton (FCC-he) collider. The hadron-hadron collider def the overall infrastructure for the FCC. With a target center-of-m energy of 100 TeV, and 16-Tesla bending magnets, such a mach will have a circumference of 100 km.

Main parameters and geometrical aspects

	LHC	FCC
Circumference [km]	26.7	100
Dipole field [T]	8.33	16
Straight sections	8 × 528 m	6 ×1400 m + 2 × 4200 m
Number of IPs	2 + 2	2 + 2
Injection energy [TeV]	0.45	3.3

FCC-hh compared with LHC and High-Luminosity LH

	LHC	HL-LHC	FCC-hh baseline		FCC-hh ultim
Energy at center of mass [TeV]	14	14	100		100
Bunch spacing [ns]	25	25	25	5	25
Number of bunches	2808	2808	10600	53000	10600
Transverse emittance [mm]	3.75	2.5	2.2	0.44	2.2
Beam current [A]	0.584	1.12	0.5		0.5
Peak luminosity [10^{34} cm^{-2}s^{-1}]	1.0	5.0	5.0		< 30.0

FCC-ee compared with the Large Electron-Positron collider (LEP2)

The main center-of-mass operating points with strong physics interest for FCC-ee a 91 GeV (Z pole), 160 GeV (W pair production threshold), 240 GeV (Higgs resonanc and 350 GeV ($t\bar{t}$ threshold).

	LEP2	FCC-ee			
		Z		W	H
Energy at center of mass [GeV]	208	91		160	240
Bunch spacing [ns]	247 / 494	7.5	2.5	50	400
Number of bunches	4	30180	91500	5260	780
Emittance (horizontal) [nm]	22	0.2	0.09	0.26	0.61
Emittance (vertical) [pm]	250	1		1	1.2
Beam current [mA]	3.04	1450		152	30
Peak luminosity (for 2 IPs) [10^{34} cm^{-2}s^{-1}]	0.012	207	90	19.1	5.1

Contacts and further information

FCC - FCC Office
fcc.office@cern.ch

EuroCirCol - Prof. Carsten P. Welsch
carsten.welsch@cockcroft.ac.uk

http://fcc.web.cern.ch

http://www.eurocircol.eu

This project has received funding from the European Union's Horizon research and innovation programme under grant No 654305. The infor herein reflects only the views of its authors and the Research Executive is not responsible for any use that may be made of the information con

Motywacja do precyzjnych badań: fabryki elektrosłabych Z, W, H, t i zapachów

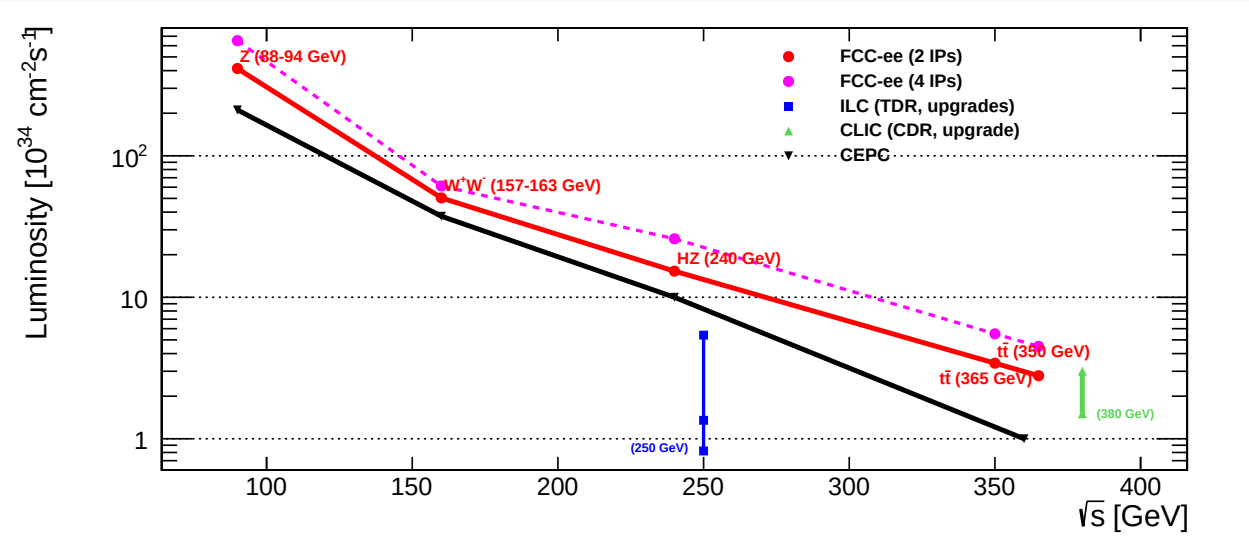

https://arxiv.org/abs/2203.06520 (z podsumowania aktywności US Snowmass)

Phase	Run duration (years)	Center-of-mass Energies (GeV)	Integrated Luminosity (ab^{-1})	Event Statistics
FCC-ee-Z	4	88-94	150	$5 \cdot 10^{12}$ **Z decays**
FCC-ee-W	2	157-163	10	10^8 WW events
FCC-ee-H	3	240	5	10^6 ZH events 25k WW $\rightarrow H$
FCC-ee-tt	5	340-365	$0.2 \div 1.5$	10^6 $t\bar{t}$ even ts 200k ZH 50k WW $\rightarrow H$

FCC-hh, optymalne dla 84 TeV pdf (referat ML Mangano)

Compositeness - badanie podstruktur cząstek elementarnych

Higgs Factories

- The Higgs boson has a size/wavelength. What's inside?

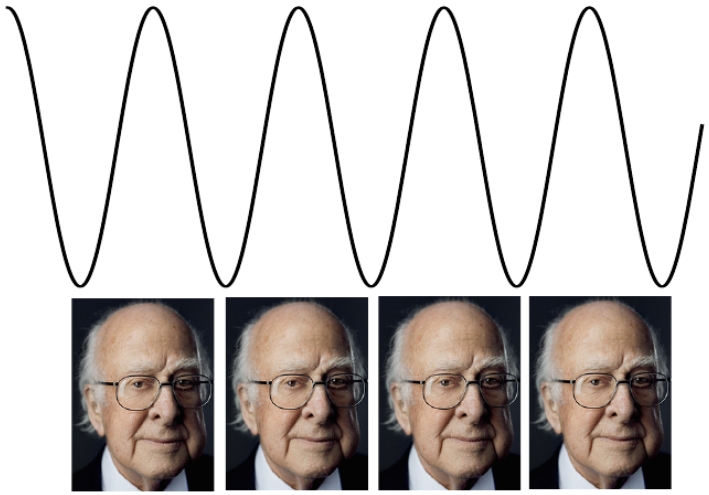

Precision measurements are different ways of probing the "compositeness of the Higgs".

$\lambda_h \approx 10^{-17}$ m

$\lambda_{10\ \mathrm{TeV}} \approx 10^{-19}$ m

Matthew Philip Mccullough, Oxford 2019,

https://indico.cern.ch/event/783429/contributions/3305140/attachments/1829729/2996092/CEPC.pdf

Referat "National Inputs" Calina Alexa, https://agenda.infn.it/event/44943/

a) Which is the preferred next major/flagship collider project for CERN?

- **Broad consensus** among CERN Member States in support of the Future Circular Collider (FCC) as a key long-term project to maintain Europe's leadership in particle physics.

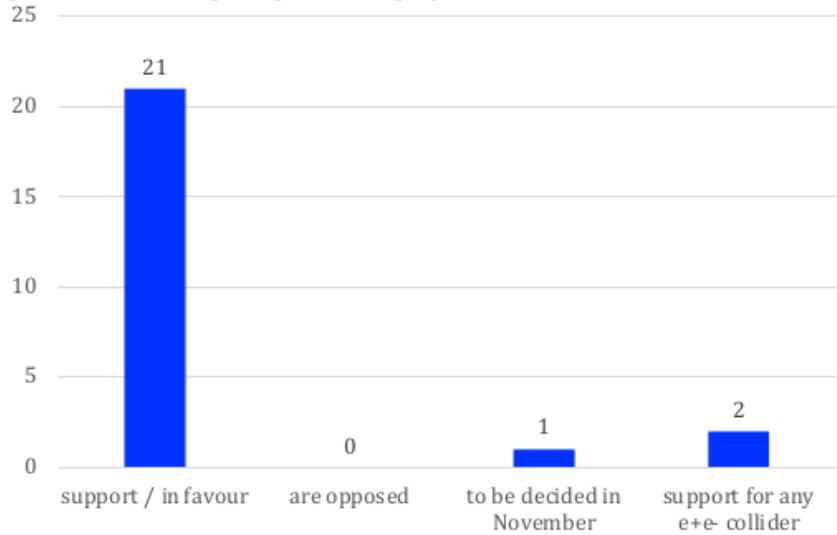

Support for FCC	Belgium, Czech Republic, Denmark, Estonia, Finland, France, Germany, Greece, Hungary, Israel, Italy, Norway, Poland, Portugal, Romania, Serbia, Slovak Republic, Spain, Sweden, Switzerland, United Kingdom
Opposed	None
To be finalized in November	Netherlands
Support for any e^+e^- collider	Austria, Bulgaria

Horizon Europe 2028-2034

16 July 2025, Commission President Ursula von der Leyen presented the Commission's proposal for the next Multiannual Financial Framework (MFF) 2028–34 and the European Competitiveness Fund (ECF), link - pdf

Based on orientation of the steering mechanism for the next MFF including the Competitiveness Coordination Tool, the Horizon Europe programme and the European Competitiveness Fund could finance a coherent sequence between research and innovation, demonstration, development and deployment, focusing efforts and funding, from the EU and national, public and private sector of 'moonshots' projects with a strong scientific component, boosting EU-wide value creation and strategic autonomy (see examples below) .
Possible 'moonshots':

- Investing in the European Organization for Nuclear Research's (CERN) Future Circular Collider, alongside other CERN's participating countries. The objective is to maintain Europe's leadership in particle physics research. The funding (up to 20% of the overall cost) could come from Horizon Europe.
- Developing Smart and Clean Aviation and European leadership in the next generation CO_2-free aircraft and automated air traffic management: It would require a partnership with industry, together with a strong scientific and engineering capacity, supported by Horizon Europe, but also a robust industrial deployment component from the Competitiveness Fund.

Moonshots

Objective: ambitious technology driven projects that boost the EU's strategic autonomy through research, development and deployment.

▸ the future circular collider ▸ clean aviation ▸ quantum computing ▸ next-generation AI ▸ data sovereignty ▸ automated transport and mobility ▸ regenerative therapies ▸ fusion energy ▸ space economy ▸ zero water pollution ▸ ocean observation

Jakiej precyzji oczekujemy na poziomie Tera-Z w FCC-ee?

$\longrightarrow 10^{12}$ rozpadów bozonu Z w rezonansie e^+e^-?

$\Longrightarrow$ 1-2 rzędy wielkości poprawa w wyznaczeniu mierzonych obserwabli!

Aby dojść do eksperymentalnej precyzji, musimy poprawić obliczenia!

Expected precision in 2040

- **Conclusion of the 2018 Workshop**

J. Gluza

> "We anticipate that, at the beginning of the FCC-ee campaign of precision measurements, the theory will be precise enough not to limit their physics interpretation. This statement is however conditional to sufficiently strong support by the physics community and the funding agencies, including strong training programmes".

- **Numerical evaluation with three-loops calculations:**

arXiv:1901.02648

	$\delta\Gamma_Z$ [MeV]	δR_l $[10^{-4}]$	δR_b $[10^{-5}]$	$\delta \sin^{2,l}_{eff}\theta$ $[10^{-6}]$
Present EWPO theoretical uncertainties				
EXP-2018	2.3	250	66	160
TH-2018	0.4	60	10	45
EWPO theoretical uncertainties when FCC-ee will start				
EXP-FCC-ee	~~0.1~~ 0.025	10	$2 \div 6$	~~6~~ 3
TH-FCC-ee	0.07	7	3	7

$0.5 \rightarrow 0.4$

Pięć lat!

- **500 person-years needed over 20 years – Recognized as strategic priority.**

President Clinton's talk at MIT's 1998 Commencement

President William Jefferson Clinton—1998 MIT Commencement

Just yesterday in Japan, physicists announced a discovery that tiny neutrinos have mass. Now, that may not mean much to most Americans, but it may change our most fundamental theories -- from the nature of the smallest subatomic particles to how the universe itself works, and indeed how it expands.

.....

The larger issue is that these kinds of findings have implications that are not limited to the laboratory. They affect the whole of society -- not only our economy, but our very view of life, our understanding of our relations with others, and our place in time.

Slajd: Kajita, Neutrino'2022, https://www.youtube.com/watch?v=9LheUWrXUHU

Niestandardowe efekty neutrin możemy też bardzo ładnie badać poprzez precyzjne pomiary i obliczenia w FCC-ee.

N_ν QED deconvolution

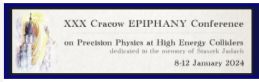

Reminder: Measuring N_ν at LEP

Phys. Rep. 427 (2006) 257

- **The Z lineshape determination**
  - Measure hadronic and leptonic cross sections (σ_{had} and $\sigma_{\ell\ell}$) as a function of E_{cm} ($\sqrt{s}$)

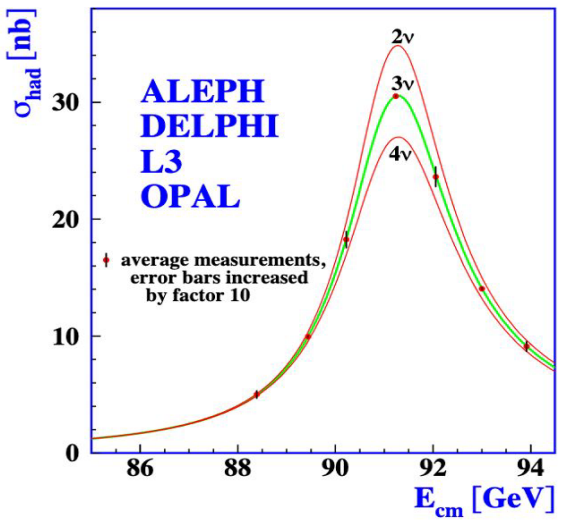

Fit to a Breit-Wigner shape
folded with QED ISR effects
Get m_Z, Γ_Z and σ^0
Get also $R^0_\ell = \sigma^0_{had} / \sigma^0_{\ell\ell}$

Staszek

KKMC, BHLUMI

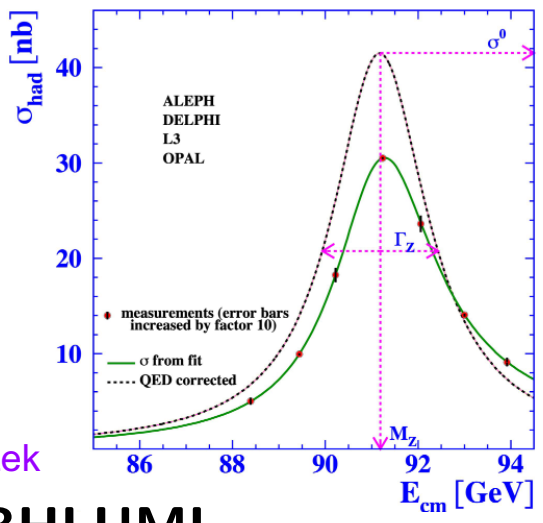

- **The peak cross section σ^0 is very sensitive to N_ν**
  - The smaller the peak cross section, the larger the number of light neutrino active species

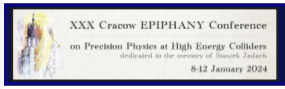

Reminder: Measuring N_ν at LEP

- **What was done in practice to extract N_ν :**
  - Total Z decay width : $\Gamma_Z = \Gamma_{ee} + \Gamma_{\mu\mu} + \Gamma_{\tau\tau} + \Gamma_{had} + N_\nu \Gamma_{\nu\nu}$
  - Divide by $\Gamma_{\ell\ell}$: $\Gamma_Z / \Gamma_{\ell\ell} = 3 + \delta_\tau + R^0_\ell + N_\nu (\Gamma_{\nu\nu} / \Gamma_{\ell\ell})$
    - δ_τ is a small phase-space correction due to the finite τ mass
    - $(\Gamma_{\nu\nu} / \Gamma_{\ell\ell})$ rather immune to SM parameters (m_{top}, m_H, …) : taken from SM
    - $\Gamma_Z / \Gamma_{\ell\ell}$ taken from Breit-Wigner peak expression
  - Solve for N_ν :

$$R^0_\ell = \frac{\Gamma_{had}}{\Gamma_{ll}}$$

$$\sigma^0_{had} = \frac{12\pi}{m_Z^2} \frac{\Gamma_{ee}\Gamma_{had}}{\Gamma_Z^2}$$

$$N_\nu \left(\frac{\Gamma_{\nu\nu}}{\Gamma_{\ell\ell}} \right)_{SM} = \left(\frac{12\pi}{m_Z^2} \frac{R^0_\ell}{\sigma^0_{had}} \right)^{\frac{1}{2}} - R^0_\ell - 3 - \delta_\tau$$

$\delta_\tau \approx -2.263.10^{-3}$

SM prediction:
= 1.99125 ± 0.00083 in 2005
= 1.99060 ± 0.00021 in 2019
Dubovik, Freitas, Gluza, Riemann,Usovitch
Phys. Lett. B 783 (2018) 86

Measured

Measured **BHLUMI**

Phys. Rep. 427 (2006) 257

XXX Cracow EPIPHANY Conference
on Precision Physics at High Energy Colliders
dedicated to the memory of Staszek Jadach
8-12 January 2024

Light fermion pair production

Four-fermion final state (with at least one e^+e^- pair) may pass the event selection

Conversion

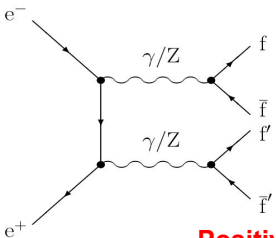

Annihilation

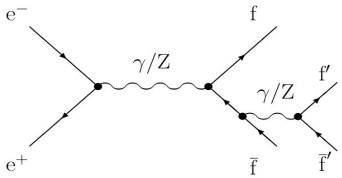

Virtual correction at the same order
(interference with tree-level graph)

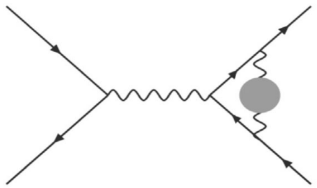

Specific four fermion MC generators

Positive correction

Negative correction

J. Gluza et al, arXiv:0807.4691
Phys. Rev. D 78 (2008) 085019

Dominant

Bremsstrahlung

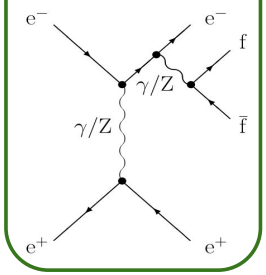

Multiperipheral

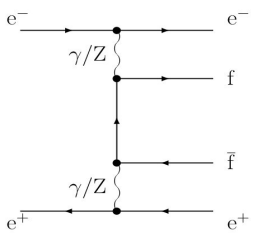

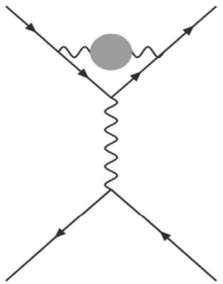

Delicate cancelation w/o cuts, but **negative correction** when selection cuts are included

(smaller momentum and larger acoplanarity angle for the e^+e^- pair in the four-fermion final state)

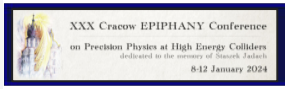

Our result made its way to the Hall of Fame in 2023

See https://pdglive.lbl.gov/
- Number of neutrino types
- Z properties (under Gauge and Higgs bosons)

Z HADRONIC POLE CROSS SECTION 41.4802 ± 0.0325 nb

OUR EVALUATION is obtained using the fit procedure and correlations as determined by the LEP Electroweak Working Group (see the note "The Z boson" and ref. LEP-SLC 2006). Corrections as discussed in VOUTSINAS 2020 and JANOT 2020 are also included.

This quantity is defined as

$$\sigma_h^0 = \frac{12\pi}{M_Z^2}\frac{\Gamma(e^+e^-)\,\Gamma(\text{hadrons})}{\Gamma_Z^2}$$

It is one of the parameters used in the Z lineshape fit.

VALUE (nb)	EVTS	DOCUMENT ID		TECN
41.4802 ± 0.0325	**OUR EVALUATION**			
41.4802 ±0.0325		[1] JANOT	2020	
• • We do not use the following data for averages, fits, limits, etc. • •				
41.500 ±0.037		[2] VOUTSINAS	2020	
41.541 ±0.037		LEP-SLC	2006	
41.501 ±0.055	4.10M	[3] ABBIENDI	2001A	OPAL
41.578 ±0.069	3.70M	ABREU	2000F	DLPH
41.535 ±0.055	3.54M	ACCIARRI	2000C	L3
41.559 ±0.058	4.07M	[4] BARATE	2000C	ALEP
42 ±4	450	ABRAMS	1989B	MRK2

[1] JANOT 2020 applies a correction to LEP-SLC 2006 using an updated Bhabha cross section calculation. account for correlated luminosity bias as presented in VOUTSINAS 2020 .

[2] VOUTSINAS 2020 applies a correction to LEP-SLC 2006 to account for correlated luminosity bias.

Number of Light ν Types 2.996 ± 0.007

(already in the PDG in 2020)

VALUE	DOCUMENT ID		TECN
2.9963 ±0.0074	[1] JANOT	2020	
• • We do not use the following data for averages, fits, limits, etc. • •			
2.9918 ±0.0081	[2] VOUTSINAS	2020	
2.9840 ±0.0082	[3] LEP-SLC	2006	RVUE

Z WIDTH 2.4955 ± 0.0023 GeV

OUR EVALUATION is obtained using the fit procedure and correlations as determined by the LEP Electroweak Working Group (see the note "The Z boson" and ref. LEP-SLC 2006). Corrections as discussed in VOUTSINAS 2020 and JANOT 2020 are also included.

VALUE (GeV)	EVTS	DOCUMENT ID		TECN	COMMENT
2.4955 ± 0.0023	**OUR EVALUATION**				
2.4955 ±0.0023		[1] JANOT	2020		
• • We do not use the following data for averages, fits, limits, etc. • •					
2.4955 ±0.0023		[2] VOUTSINAS	2020		
2.4952 ±0.0023		LEP-SLC	2006		$E_{cm}^{ee} = 88 - 94$ GeV

$N_\nu = 2.9963 \pm 0.0074$ - "wirtualny" ślad "nowej fizyki"!
Świetny przykład połączenia teorii (nasze obliczenia NNLO plus BHLUMI) i eksperymentalna analiza danych.

Flagowy przykład precyzyjnej fizyki w fizyce wysokich energii e^+e^-:

wierzchołek $Zf\bar{f}$ i poprawki elektrosłabe

1986

1993-2014

2016-2019

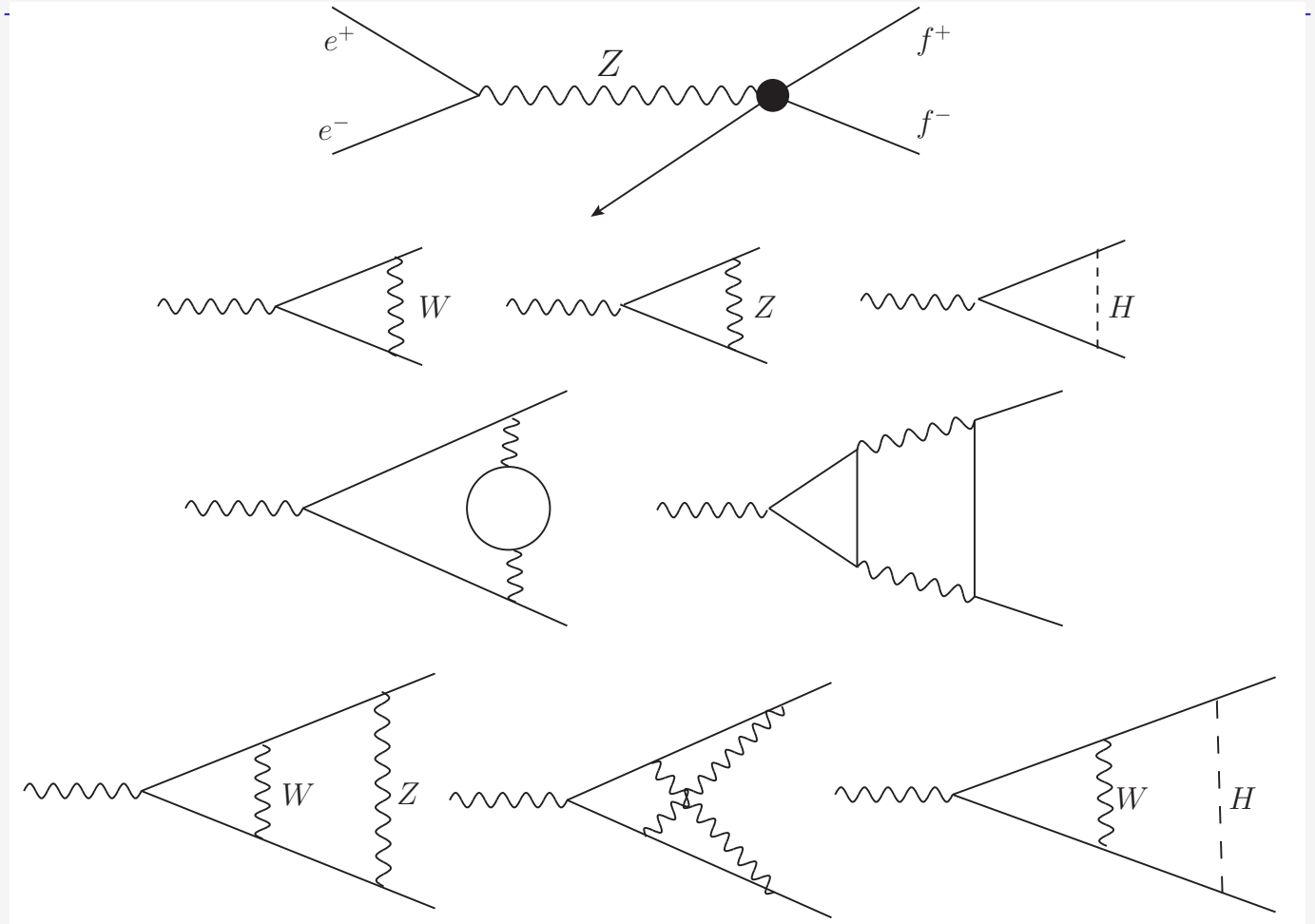

I. Dubovyk, A. Freitas, JG, T. Riemann, J. Usovitsch,
https://doi.org/10.1016/j.physletb.2016.09.012
https://doi.org/10.1016/j.physletb.2018.06.037
https://doi.org/10.1007/JHEP08(2019)113

SM precision needed for discovery studies (indirect effects)

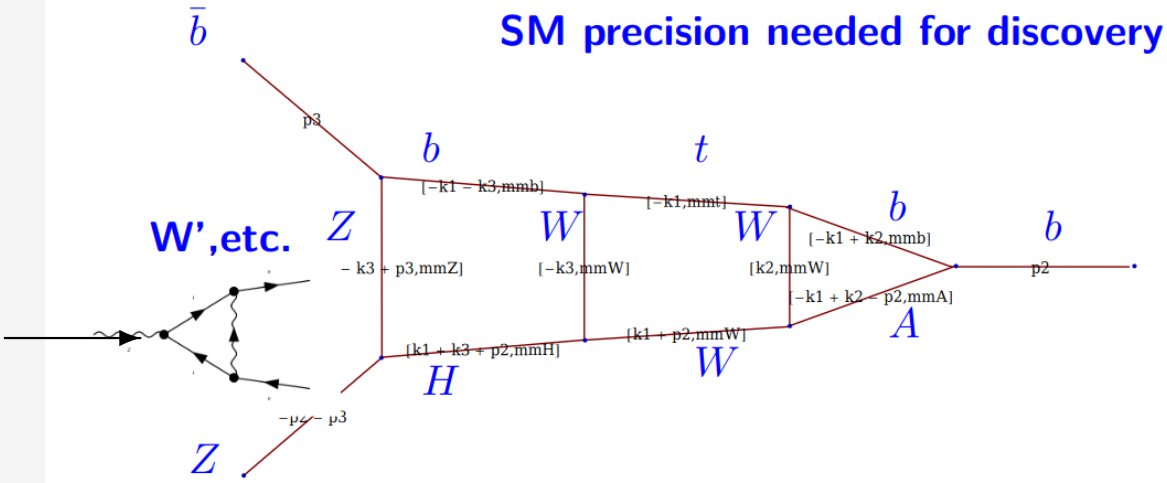

Four scales :

$$\left\{ \frac{M_H^2}{M_Z^2}, \frac{M_W^2}{M_Z^2}, \frac{m_t^2}{M_Z^2}, \frac{s+i\varepsilon}{M_Z^2} \right\}$$

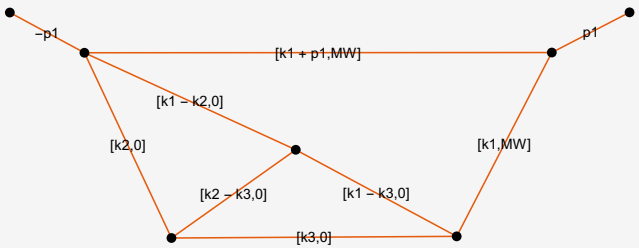

1-dim

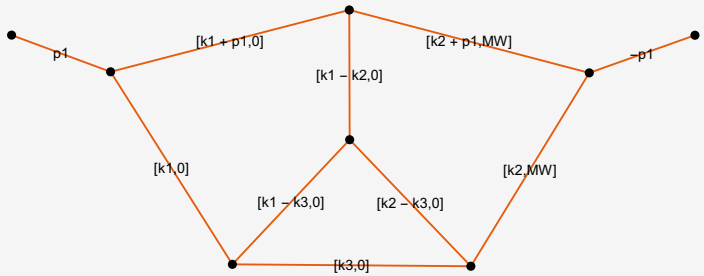

4-dim

$$-18.779406962 - 6.390785027i \qquad -22.5213 + 4.74442i \pm (0.001 + 0.001i)$$

$$I = -\frac{1}{(-s)^{1+3\epsilon}} \int_{-i\infty}^{+i\infty} \prod_{i=1}^{4} dz_i \left(-\frac{M_W^2}{s}\right)^{z_3} \frac{\Gamma(-\epsilon - z_1)\Gamma(-z_1)\Gamma(1+2\epsilon+z_1)}{\Gamma(1-2\epsilon)\Gamma(1-3\epsilon-z_1)}$$
$$\times \frac{\Gamma(-2\epsilon - z_{12})\Gamma(1-\epsilon+z_2)\Gamma(1+z_{12})\Gamma(1+\epsilon+z_{12})\Gamma(1+3\epsilon+z_3)\Gamma(1-\epsilon-z_4)}{\Gamma(1-z_2)\Gamma(2+\epsilon+z_{12})} \ldots$$

Reprezentacje Mellin-Barnesa w HEP - metoda

- "Om definita integraler", R. H. Mellin, Acta Soc. Sci. Fenn. 20(7), 1 (1895),
  "The theory of the gamma function", E. W. Barnes Messenger Math. 29(2), 64 (1900).

$$matematyka \longrightarrow \frac{1}{(A+B)^{\lambda}} = \frac{1}{\Gamma(\lambda)}\frac{1}{2\pi i}\int_{-i\infty}^{+i\infty} dz\Gamma(\lambda+z)\Gamma(-z)\frac{B^z}{A^{\lambda+z}}$$

$$fizyka \longrightarrow \frac{1}{(p^2-m^2)^{a}} = \frac{1}{\Gamma(a)}\frac{1}{2\pi i}\int_{-i\infty}^{+i\infty} dz\Gamma(a+z)\Gamma(-z)\frac{(m^2)^z}{(p^2)^{a+z}}$$

Rekurencja $\Longrightarrow$ wielowymiarowe zespolone całki.

$$\frac{1}{(A_1+\ldots+A_n)^{\lambda}} = \frac{1}{\Gamma(\lambda)}\frac{1}{(2\pi i)^{n-1}}\int_{-i\infty}^{i\infty} dz_1\ldots dz_{n-1}$$
$$\times\prod_{i=1}^{n-1} A_i^{z_i}\; A_n^{-\lambda-z_1-\ldots-z_{n-1}}\prod_{i=1}^{n-1}\Gamma(-z_i)\;\Gamma(\lambda+z_1+\ldots+z_{n-1})$$

Analityczne i numeryczne obliczanie całek Mellin-Barnesa

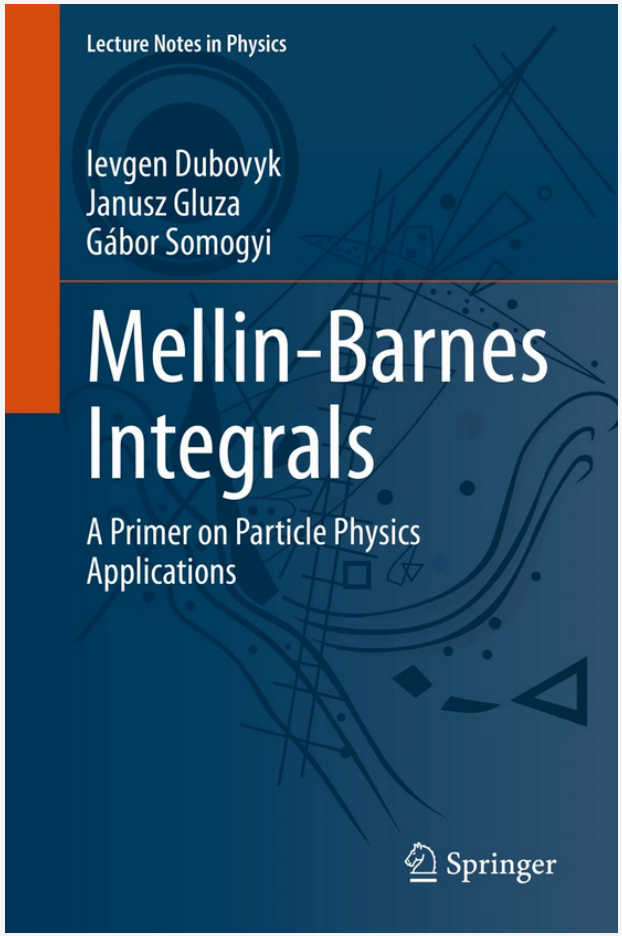

6 MB Numerical Methods . . . 221
6.1 Introduction . . . 221
6.2 MB Numerical Evaluation Using Bromwich Contours . . . 225
6.2.1 Straight Line Contours and Their Limitations . . . 225
6.2.2 Transforming Variables to the Finite Integration Range . . . 227
6.2.3 Shifting and Deforming Contours of Integration . . . 230
6.2.4 Thresholds and no Need for Contour Deformations . . . 232
6.3 MB Numerical Evaluation by Steepest Descent . . . 235
6.3.1 General Idea . . . 236
6.3.2 Implementation of the Method . . . 238
6.3.3 Tricks and pitfalls for 'Vanishing Derivatives' . . . 241
6.3.4 Beyond One-dimensional Cases . . . 243
6.4 Numerical evaluation of phase space MB integrals . . . 244
Problems . . . 248
References . . . 249

A Public Software and Codes For MB Studies . . . 253
A.1 Analytic software . . . 253
A.2 Multiple sums . . . 254
A.3 Polylogarithms and generalizations . . . 255
A.4 MB numerical software . . . 256
A.5 Other methods for FI numerical integrations . . . 257

B Additional Working Files . . . 259

https://arxiv.org/abs/2211.13733
https://doi.org/10.1007/978-3-031-14272-7

Fizyka zderzaczy ... magia świata matematyki

$$T = 2\pi\sqrt{\frac{l}{g}} \times {}_2F_1\left[\frac{1}{2}, \frac{1}{2}; 1; \sin^2\theta\right]$$

Rozwiazania analityczne dla masywnych całek wielopetlowych, opisujacych procesy/rozpady rozpraszania, wykraczaja poza funkcje eliptyczne – jak daleko?

Symboliczne, numeryczne rozwiązania:
Wielkie wyzwania na dekady!

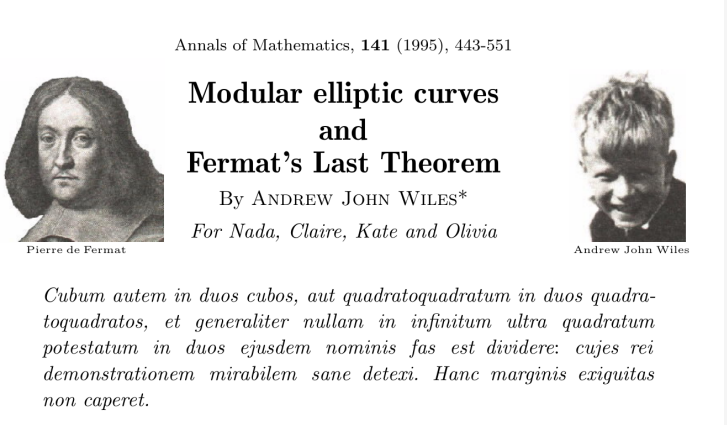

Annals of Mathematics, **141** (1995), 443-551

Modular elliptic curves and Fermat's Last Theorem

By Andrew John Wiles*

For Nada, Claire, Kate and Olivia

Pierre de Fermat

Andrew John Wiles

Cubum autem in duos cubos, aut quadratoquadratum in duos quadratoquadratos, et generaliter nullam in infinitum ultra quadratum potestatum in duos ejusdem nominis fas est dividere: cujes rei demonstrationem mirabilem sane detexi. Hanc marginis exiguitas non caperet.

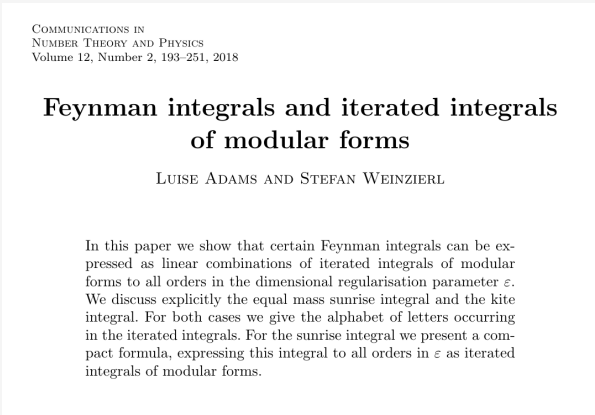

Communications in Number Theory and Physics
Volume 12, Number 2, 193–251, 2018

Feynman integrals and iterated integrals of modular forms

Luise Adams and Stefan Weinzierl

In this paper we show that certain Feynman integrals can be expressed as linear combinations of iterated integrals of modular forms to all orders in the dimensional regularisation parameter ε. We discuss explicitly the equal mass sunrise integral and the kite integral. For both cases we give the alphabet of letters occurring in the iterated integrals. For the sunrise integral we present a compact formula, expressing this integral to all orders in ε as iterated integrals of modular forms.

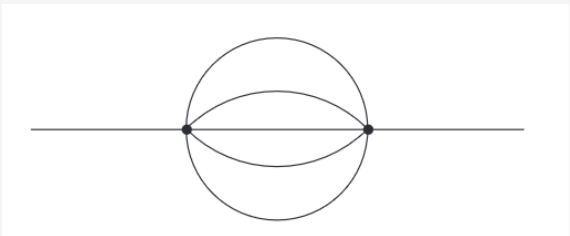

"Epsilon-factorized form" of banana 4-loop integrals $\rightarrow$ fast evaluations to nearly arbitrary precision.

'Taming Calabi-Yau Feynman Integrals: The Four-Loop Equal-Mass Banana Integral', S. Pögel, X. Wang, S. Weinzierl,

Trzy wiodące metody obliczeń (analityczne oraz numeryczne)

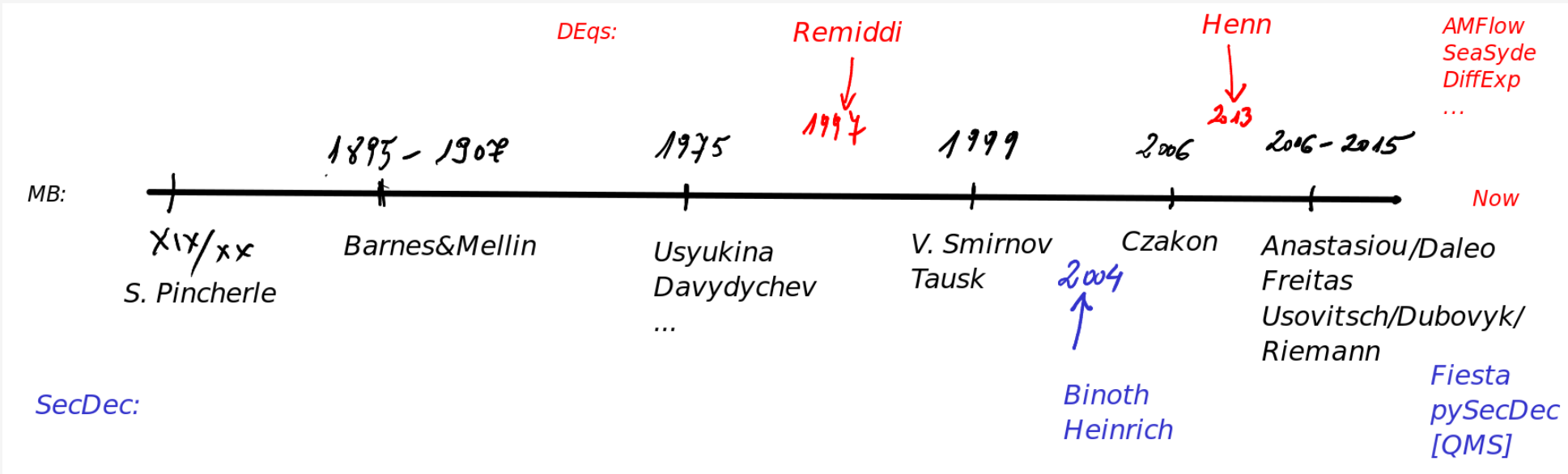

Analityczne rozwiązania, przykład rozpraszanie Bhabhy $e^+e^- \to e^+e^-$

$$G(X) = \frac{1}{\left(i\pi^{d/2}\right)^L} \int \frac{d^d k_1 \ldots d^d k_L \quad X}{(q_1^2 - m_1^2)^{\nu_1} \ldots (q_j^2 - m_j^2)^{\nu_j} (q_N^2 - m_N^2)^{\nu_N}},$$

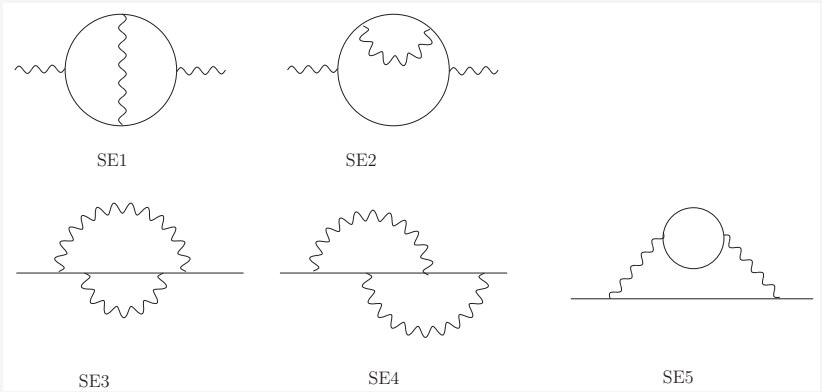

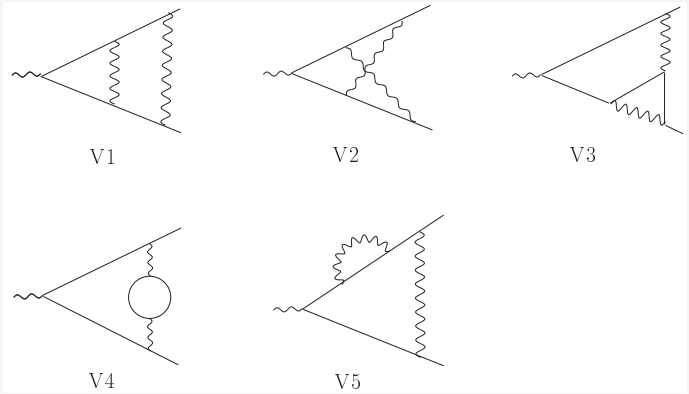

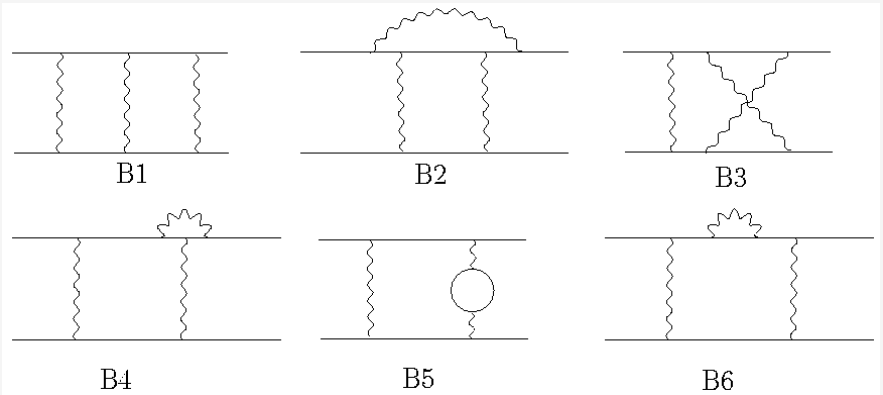

Rozpraszanie Bhabhy $e^+e^- \to e^+e^-$

energy kernel is trivial, $K_{\rm SE}(z) = 1/(q^2 - z)$. Whereas the two-loop vertex kernel K_v can be found in Eq. (5) of [15], the cross-section corrections due to the double boxes of Fig. 1(c) depend on three such kernels $K_a(z)$, $a = A, B, C$ [12,16]. Notice that, unlike the vertex kernel, the box kernels are infrared divergent, but, analogously to the one-loop box, they have no singularity in the electron mass. The net cross-section contribution from the eight double box diagrams is still infrared divergent. These boxes become, as well as the reducible diagrams with one-loop vertices and boxes, infrared finite after adding real soft photon emission. The anatomy of that is nicely detailed in Section 2.2 of [7]. In order to construct an infrared-finite quantity, we combine: (i) Born diagrams interfering with the two-loop box diagrams [Fig. 1(c)] and with reducible vertices [Fig. 1(b)], (ii) Born diagrams with a one-loop vacuum polarization function interfering with single one-loop boxes and vertices, and finally (iii) real single-photon emission with a one-loop vacuum polarization [18]. The resulting cross section becomes

$$\frac{d\bar{\sigma}}{d\Omega} = c\int_{4M_\pi^2}^{\infty} dz \frac{R_{\rm had}(z)}{z}\frac{1}{t-z}F_1(z) + c\int_{4M_\pi^2}^{\infty}\frac{dz}{z(s-z)}\left\{R_{\rm had}(z)\left[F_2(z) + F_3(z)\ln\left|1-\frac{z}{s}\right|\right] - R_h(s)\left[F_2(s) + F_3(s)\ln\left|1-\frac{z}{s}\right|\right]\right\}$$
$$+ c\frac{R_h(s)}{s}\left\{F_2(s)\ln\left(\frac{s}{4M_\pi^2}-1\right) - 6\zeta_2 F_a(s) + F_3(s)\left[2\zeta_2 + \frac{1}{2}\ln^2\left(\frac{s}{4M_\pi^2}-1\right) + \mathrm{Li}_2\left(1-\frac{s}{4M_\pi^2}\right)\right]\right\}, \tag{5}$$

with $c = \alpha^4/(\pi^2 s)$ and $R_h(s) = \theta(s - 4M_\pi^2)R_{\rm had}(s)$. Further,

$$F_1(z) = \frac{1}{3}\left\{9\bar{c}(s,t)\ln\left(\frac{s}{m_e^2}\right) + \left[-z^2\left(\frac{1}{s}+\frac{2}{t}+2\frac{s}{t^2}\right) + z\left(4+4\frac{s}{t}+2\frac{t}{s}\right) + \frac{1}{2}\frac{t^2}{s} + 6\frac{s^2}{t} + 5s + 4t\right]\ln\left(-\frac{t}{s}\right) + s\left(-\frac{z}{t}+\frac{3}{2}\right)\right.$$
$$\times\ln\left(1+\frac{t}{s}\right) + \left[\frac{1}{2}\frac{z^2}{s} + 2z\left(1+\frac{s}{t}\right) - \frac{11}{4}s - 2t\right]\ln^2\left(-\frac{t}{s}\right) - \left[\frac{1}{2}\frac{z^2}{t} - z\left(1+\frac{s}{t}\right) + \frac{t^2}{s} + 2\frac{s^2}{t} + \frac{9}{2}s + \frac{15}{4}t\right]$$
$$\times\ln^2\left(1+\frac{t}{s}\right) + \left[\frac{z^2}{t} - 2z\left(1+\frac{s}{t}\right) + 2\frac{s^2}{t} + 5s + \frac{5}{2}t\right]\ln\left(-\frac{t}{s}\right)\ln\left(1+\frac{t}{s}\right) - 4\left[\frac{t^2}{s} + 2\frac{s^2}{t} + 3(s+t)\right]$$
$$\times\left[1 + \mathrm{Li}_2\left(-\frac{t}{s}\right)\right] - \left[\frac{t^2}{s} + 2\frac{s^2}{t} + 3(s+t)\right]\ln\left(\frac{z}{s}\right)\ln\left(1+\frac{t}{s}\right) - \left[2\frac{z^2}{t} - 4z\left(1+\frac{s}{t}\right) - 4\frac{t^2}{s} - 2\frac{s^2}{t} + s - \frac{11}{2}t\right]\zeta_2$$
$$+\left[z^2\left(\frac{1}{s}+2\frac{s}{t^2}+\frac{2}{t}\right) - z\left(\frac{t}{s}+2\frac{s}{t}+2\right)\right]\ln\left(\frac{z}{s}\right) - \left[z^2\left(\frac{1}{s}+\frac{1}{t}\right) + 2z\left(1+\frac{s}{t}\right) + s + 2\frac{s^2}{t}\right]\ln\left(\frac{z}{s}\right)\ln\left(1+\frac{z}{s}\right)$$
$$+\left[\frac{z^2}{s} + 4z\left(1+\frac{s}{t}\right) - \frac{t^2}{s} - 4(s+t)\right]\ln\left(\frac{z}{s}\right)\ln\left(1-\frac{z}{t}\right) - \left[z^2\left(\frac{1}{s}+2\frac{s}{t^2}+\frac{2}{t}\right) - 2z\left(\frac{t}{s}+2\frac{s}{t}+2\right) + \frac{t^2}{s} + 2(s+t)\right]$$
$$\times\ln\left(1-\frac{z}{t}\right) + \left[\frac{z^2}{t} - 2z\left(1+\frac{s}{t}\right) + 2\frac{t^2}{s} + 8s + 4\frac{s^2}{t} + 7t\right]\ln\left(1-\frac{z}{t}\right)\ln\left(1+\frac{t}{s}\right) + \left[\frac{z^2}{s} + 4z\left(1+\frac{s}{t}\right) - \frac{t^2}{s} - 4(s+t)\right]$$
$$\times\mathrm{Li}_2\left(\frac{z}{t}\right) - \left[z^2\left(\frac{1}{s}+\frac{1}{t}\right) + 2z\left(1+\frac{s}{t}\right) + s + 2\frac{s^2}{t}\right]\mathrm{Li}_2\left(-\frac{z}{s}\right) - \left[\frac{z^2}{t} - 2z\left(1+\frac{s}{t}\right) + \frac{t^2}{s} + 5s + 2\frac{s^2}{t} + 4t\right]$$
$$\left.\times\mathrm{Li}_2\left(1+\frac{z}{u}\right)\right\} + 4\bar{c}(s,t)\ln\left(\frac{2\omega}{\sqrt{s}}\right)\left[\ln\left(\frac{s}{m_e^2}\right) + \ln\left(-\frac{t}{s}\right) - \ln\left(1+\frac{t}{s}\right) - 1\right], \tag{6}$$

Harmoniczne polilogarytmy

$$
\begin{aligned}
H(0;x) &= \ln x \ , \\
H(1;x) &= \int_0^x \frac{dx'}{1-x'} = -\ln(1-x) \ , \\
H(-1;x) &= \int_0^x \frac{dx'}{1+x'} = \ln(1+x)
\end{aligned}
$$

$$
\begin{aligned}
H(\vec{0}_w;x) &= \frac{1}{w!}\ln^w x \\
H(\vec{m}_w;x) &= \int_0^x dx' \ f(a;x') \ (\vec{m}_{w-1};x')
\end{aligned}
$$

Proces Bhabhy, prosty alfabet i litery (tylko 3):

$$
f(0,x) = \frac{1}{x}, \quad f(1,x) = \frac{1}{1-x}, \quad f(-1,x) = \frac{1}{1+x}
$$

Harmoniczne polilogarytmy

$$
\begin{aligned}
H(0;x) &= \ln x \ , H(0,0;x) = \int \frac{H[0,x]}{x} dx = \frac{1}{2!} \ln^2 x, ... \\
H(1;x) &= \int_0^x \frac{dx'}{1-x'} = -\ln(1-x) \ , \\
H(-1;x) &= \int_0^x \frac{dx'}{1+x'} = \ln(1+x) \\
H(0,1;x) &= \int_0^x \frac{dx'}{x'} H(1;x') = -\int_0^x \frac{dx'}{x'} \ln(1-x') \ , \\
H(0,1;x) &= {}_2(x) \ , \\
H(1,0;x) &= \int_0^x \frac{dx'}{1-x'} H(0;x') = \int_0^x \frac{dx'}{1-x'} \ln x'
\end{aligned}
$$

$$
\begin{aligned}
H(1,0;x) &= \int_0^x \frac{dx'}{1-x'} H(0;x') = \int_0^x \frac{dx'}{1-x'} \ln x' \ , \\
H(1,0;x) &= -\ln x \ln(1-x) +_2 (x) \\
H(1,0;x) &= H(0,x)H(1,x) - H(0,1;x)
\end{aligned}
$$

$$
\begin{aligned}
H(\vec{a},x)H(\vec{b},x) &= \sum_{\vec{c}=\vec{a}+\vec{b}} H(\vec{c},x) \\
H(m_1,...,m_q,x) &= H(m_1,x)H(m_2,...,m_q,x) \\
&\quad -H(m_1,m_2,x)H(m_3,...,m_q,x) \\
&\quad +... + (-1)^{q+1} H(m_q,...,m_1,x)
\end{aligned}
$$

Two-Loop Integrals — Hexabox Topology

$$\mathrm{d}I = \epsilon\,\mathbf{M}\,I\,, \qquad \mathbf{M} = M_\alpha\,\mathrm{d}\log W_\alpha$$

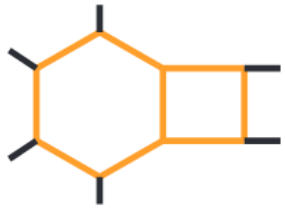

- **202 master integrals**, in 126 different sectors
  - 185 are five-point one-mass topologies. All this for 17 new integrals!
- **128 letters**, only 11 new ones (associated with six-point topologies)
  - 9 appear in the differential equation on the maximal cut, 2 appear in the off-shell penta-triangle
  - 2 `off-shell letters' are odd under $\sqrt{\Delta_5}$, 9 `on-shell' letters are even
- Closure of the alphabet under dihedral symmetry: **245 letters**
- From here we know how to proceed to get basis of functions, evaluate integrals, …

Rodzaje diagramów

Mamy więc ciekawe topologicznie struktury diagramów Feynmana i odpowiadajace im całki, np. sunrise (sunset), mercedes, crown, neckles, ladder, ...,

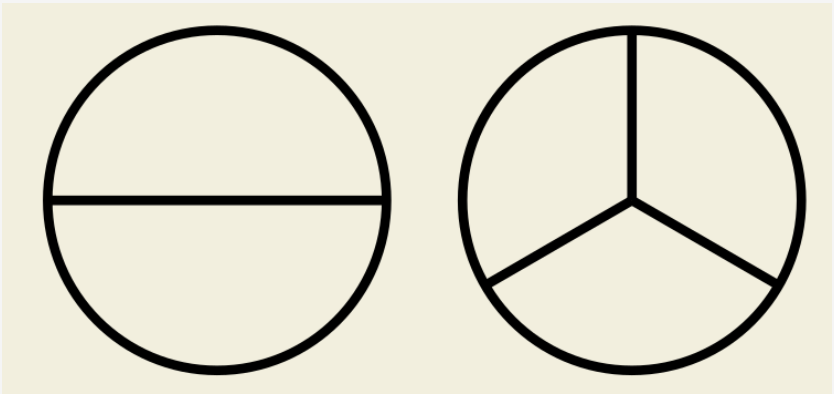

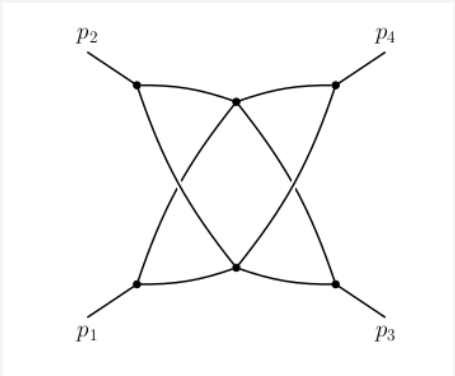

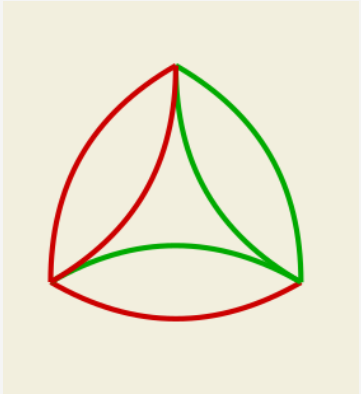

W przypadku analitycznych rozwiazań mamy wielo-literowe alfabety do znajdywania matematycznych funkcji im odpowiadajacych.

I numerycznie: Wielopętlowe obliczenia, rozbieżności, renormalizacja ...

$$\Big(\text{YInt}(\text{dd}(\text{k1}, 0), \text{dd}(\text{k2}, 0), \text{dd}(\text{k1} + \text{k2}, 0), \text{dd}(\text{k2} - \text{p1}, 0), \text{dd}(\text{k1} + \text{p1}, 0), \text{dn2}(\text{k1 k2}), \text{dn2}(\text{k1 k2})) \to (-13.627371194393887714109343\mathit{83} + 20.166895843892192345339\mathit{1}$$

$$(11.493518704663773474947860\mathit{09} - 21.854216824115801472400370\mathit{42}\, i)\, \text{eps}^2 + (1.010805534687752347048684\mathit{410} + 8.050331174823845173560523\mathit{670}\, i)\, \text{eps} +$$

$$(1.281250000000000000000000\mathit{00} + 1.178097245096172464423491\mathit{269}\, i) + \frac{0.187500000000000000000000\mathit{00} + 0.\times 10^{-29}\, i}{\text{eps}}\Big),$$

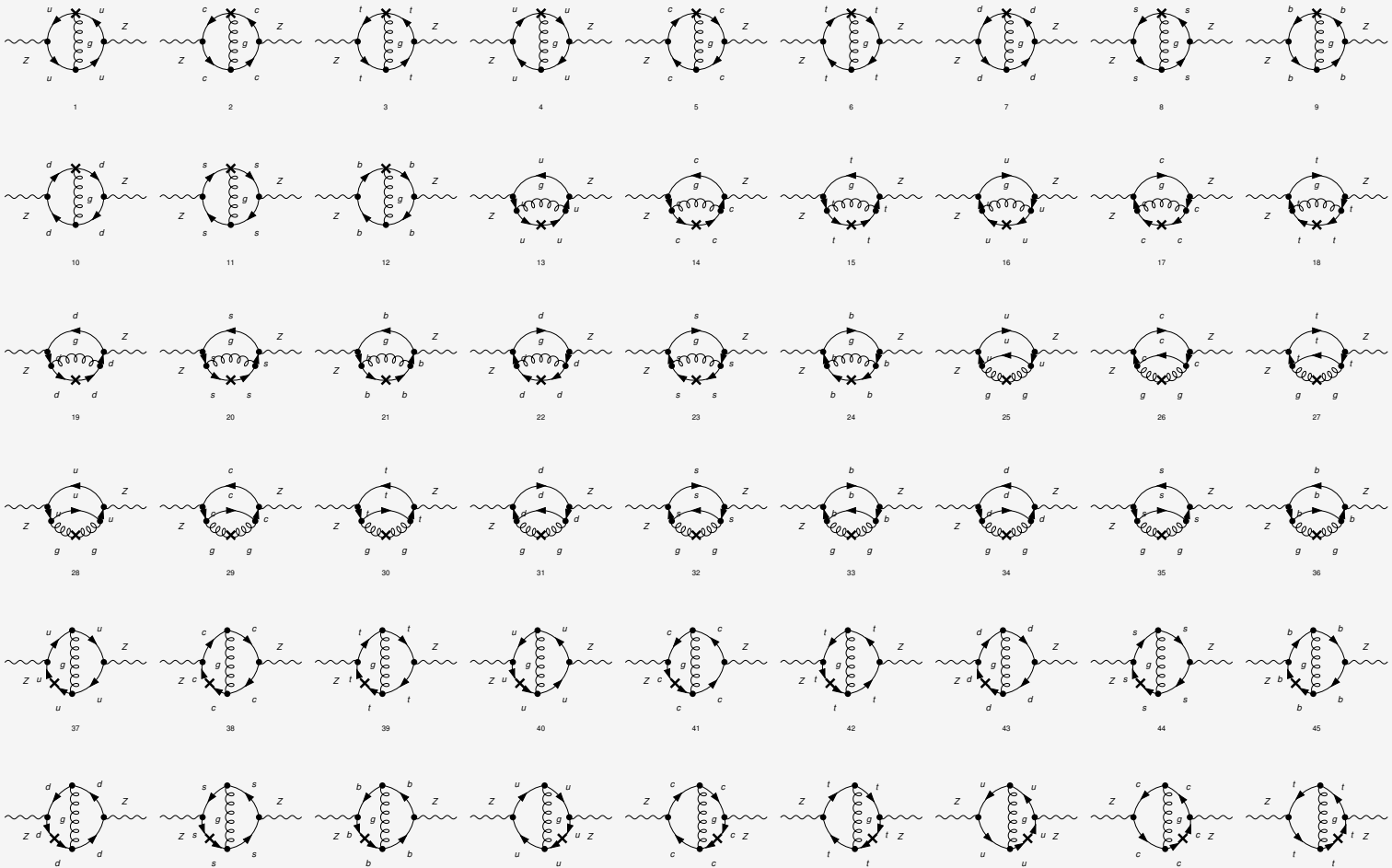

Zamiast podsumowania

"in this field, almost everything is already discovered, and all that remains is to fill a few unimportant holes"

Philipp von Jolly
(1809-1884)

advice to the young Max Planck
not to go into physics, Munich 1878

Albert Michelson (1894):

"It seems probable that most of the grand underlying principles have been firmly established (...) the future truths of physical science are to be looked for in the sixth place of decimals"

Q: Dear Albert: What about special and general relativity, and quantum mechanics, particle physics, ...?

Dziękuję za uwagę.

Dodatkowe slajdy

$$F = k\frac{qQ}{r^2} \equiv \frac{1}{4\pi\epsilon_0}\frac{qQ}{r^2} \quad \rightarrow \alpha \equiv \frac{\phi \mathbf{e}}{\mathbf{mc^2}} = \frac{\frac{\mathbf{e^2}}{\mathbf{4\pi\epsilon_0 L}}}{\mathbf{mc^2}} = \frac{\mathbf{e^2}}{\mathbf{4\pi\epsilon_0 \hbar c}},\ L = \frac{\hbar}{mc}$$

Stała struktury subtelnej α wynosi liczbowo około 1/137 [137.035999206(11)]

Czy 1/136 lub 1/138 robi różnicę?

Procentowe zmiany w wartości α implikuja czerwone lub niebieskie gwiazdy ("Gravitation", Misner, Thorne, Wheeler)

F. Zimmermann, 11th FCC-ee Workshop, CERN, January 2019

https://indico.cern.ch/event/766859

---

vertical spot size challenge

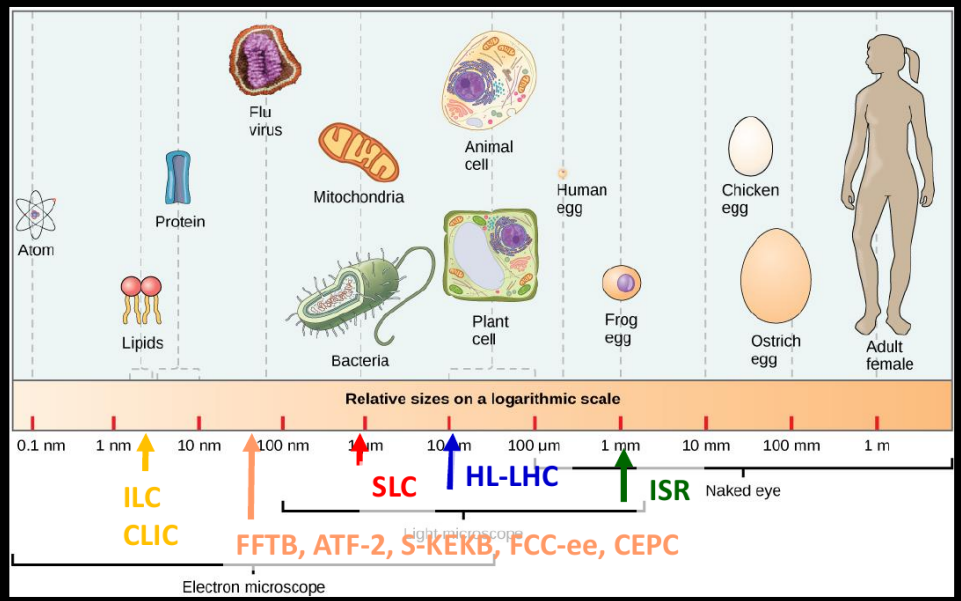

FCC-ee in the regime of FFTB, ATF-2, and especially SuperKEKB

J. Wenniger, LEP Fest 2000, https://indico.cern.ch/event/408341/

Moonrise over LEP

Fall of 1992 : The historic tide experiment !

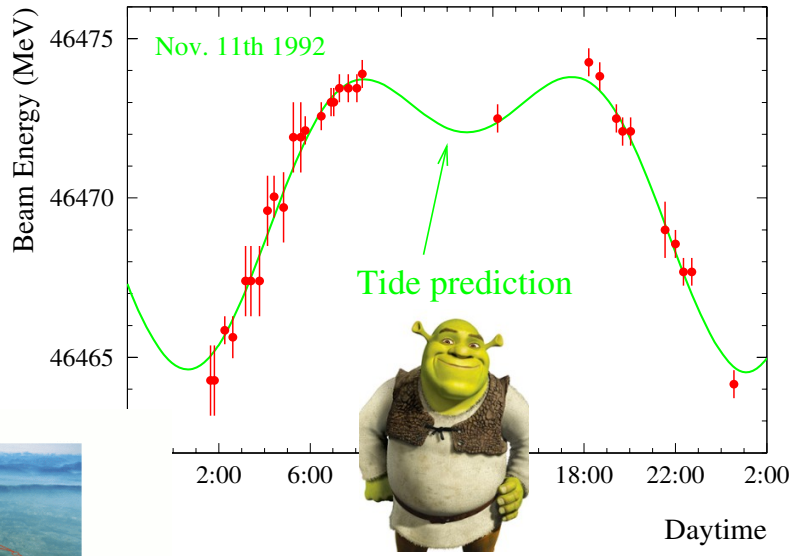

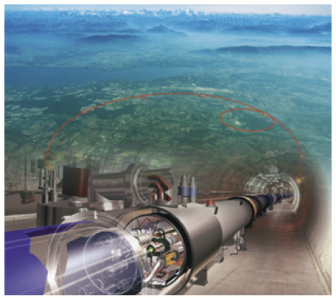

total strain is 4 x 10^{-8} (ΔC = 1 mm)

Aby dojść do eksperymentalnej precyzji, musimy poprawić obliczenia!

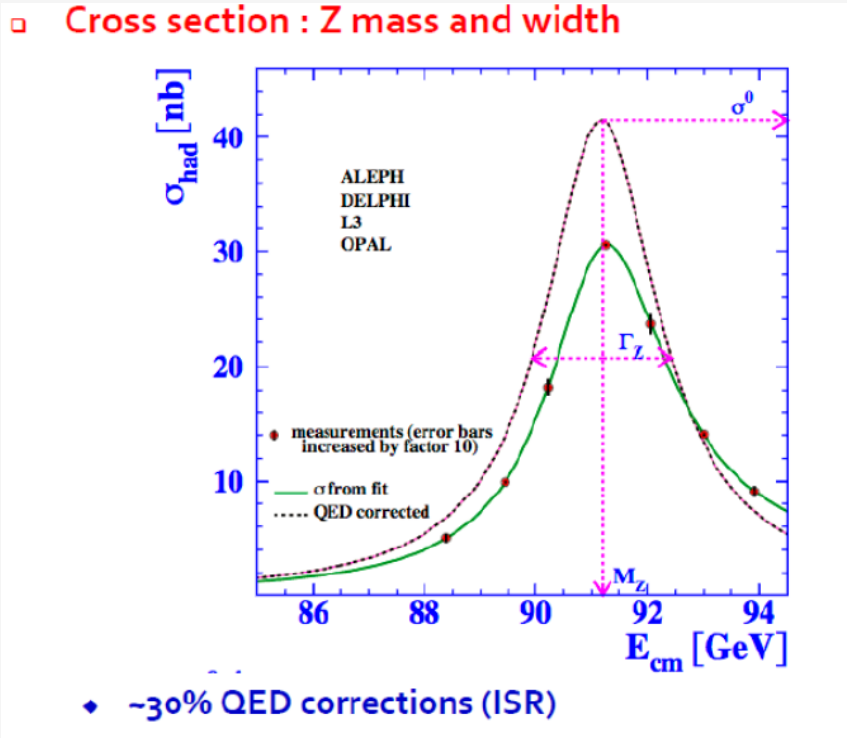

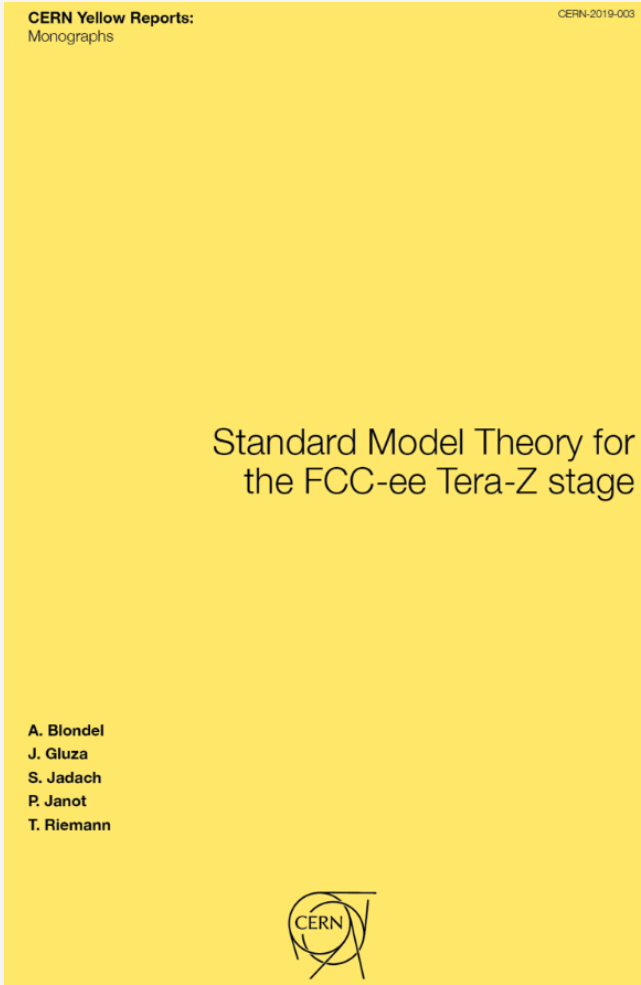

$$\frac{\delta\Gamma_Z}{\Gamma_Z} = \frac{.025}{2495} \simeq 10^{-5}!$$

A. Blondel, P. Janot, 2106.13885

Observable	present value ± error	FCC-ee **Stat.**	FCC-ee Syst.	Comment and leading exp. error
m_Z (keV)	91186700 ± 2200	**4**	100	From Z line shape scan Beam energy calibration
Γ_Z (keV)	2495200 ± 2300	**4**	25	From Z line shape scan Beam energy calibration
$\sin^2\theta_W^{\rm eff}(\times 10^6)$	231480 ± 160	**2**	2.4	from $A_{FB}^{\mu\mu}$ at Z peak Beam energy calibration
$1/\alpha_{QED}(m_Z^2)(\times 10^3)$	128952 ± 14	**3**	small	from $A_{FB}^{\mu\mu}$ off peak QED&EW errors dominate
R_ℓ^Z $(\times 10^3)$	20767 ± 25	**0.06**	0.2-1	ratio of hadrons to leptons **acceptance for leptons**
$\alpha_s(m_Z^2)$ $(\times 10^4)$	1196 ± 30	**0.1**	0.4-1.6	from R_ℓ^Z above
σ_{had}^0 $(\times 10^3)$ (nb)	41541 ± 37	**0.1**	4	peak hadronic cross section luminosity measurement
$N_\nu(\times 10^3)$	2996 ± 7	**0.005**	1	Z peak cross sections Luminosity measurement
R_b $(\times 10^6)$	216290 ± 660	**0.3**	< 60	ratio of $b\bar{b}$ to hadrons stat. extrapol. from SLD
$A_{FB}^{b,0}$ $(\times 10^4)$	992 ± 16	**0.02**	1-3	b-quark asymmetry at Z pole from jet charge
$A_{FB}^{pol,\tau}$ $(\times 10^4)$	1498 ± 49	**0.15**	<2	τ polarization asymmetry τ decay physics
τ lifetime (fs)	290.3 ± 0.5	**0.001**	0.04	radial alignment
τ mass (MeV)	1776.86 ± 0.12	**0.004**	0.04	momentum scale
τ leptonic ($\mu\nu_\mu\nu_\tau$) B.R. (%)	17.38 ± 0.04	**0.0001**	0.003	e/μ/hadron separation
m_W (MeV)	80350 ± 15	**0.25**	0.3	From WW threshold scan Beam energy calibration

Doskonały pomiar energii środka masy poprzez rezonansową depolaryzację wiązek pilotujących

PRECISION

LHC and HL-LHC

HL-LHC aims at percent precision

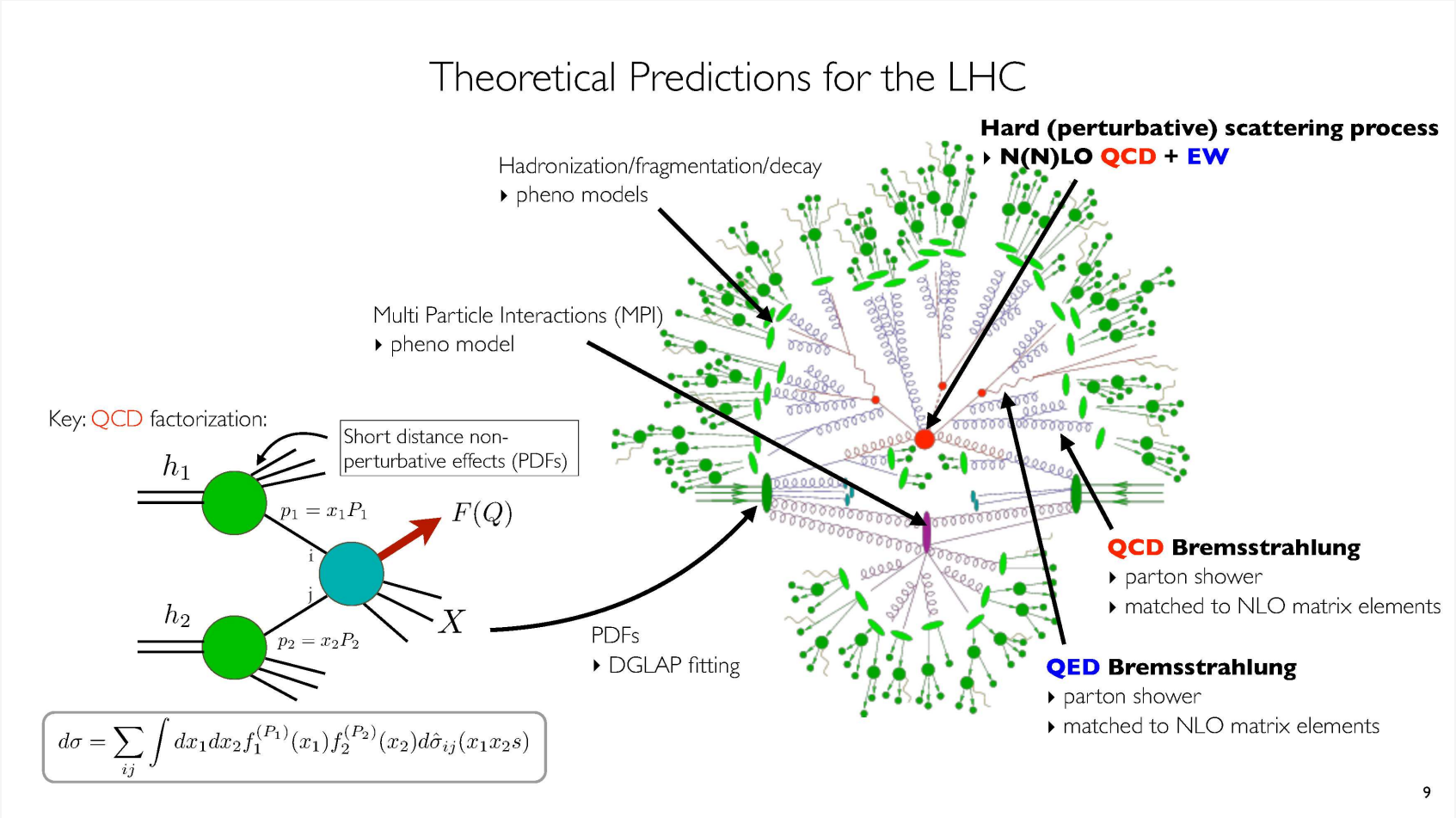

"Standard Model Theory, Jonas M. Lindert, EPS 2021, https://indico.desy.de/event/28202

Od 2012 roku: stały wzrost precyzji, szeroka gama procesów

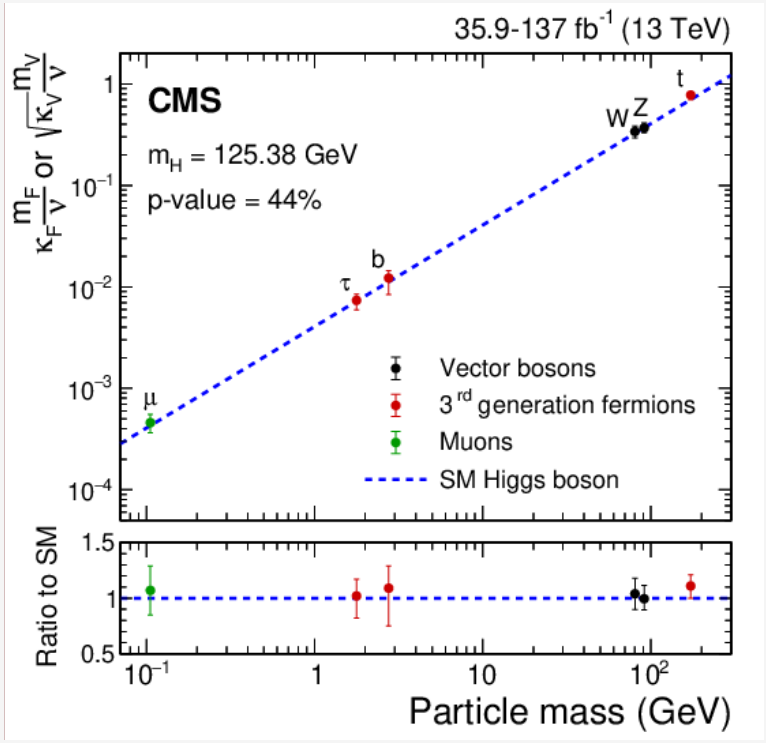

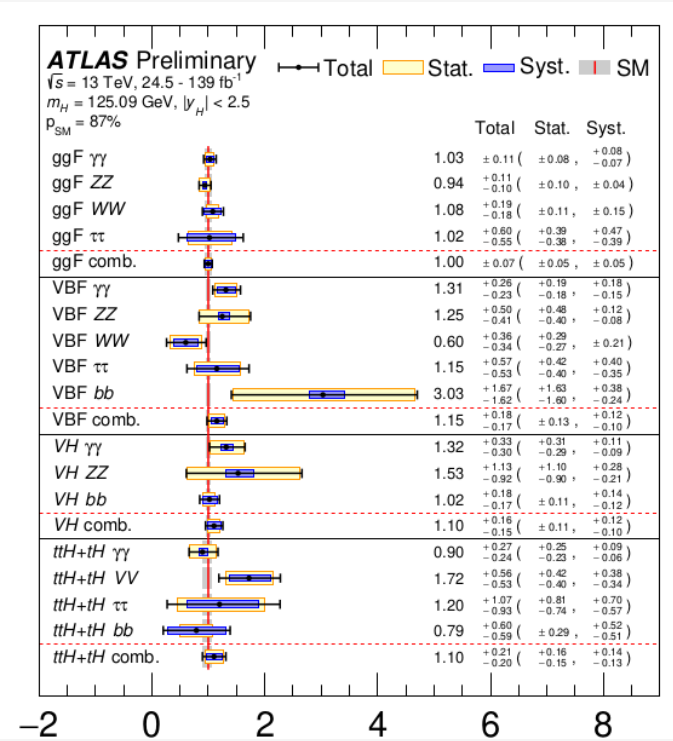

ATLAS 2020: https://cds.cern.ch/record/2725733
CMS 2020: http://cds.cern.ch/record/2730058

Workshop: Precision calculations for future e^+e^- colliders: targets and tools,

CERN 2022, talk by V. Sotnikov

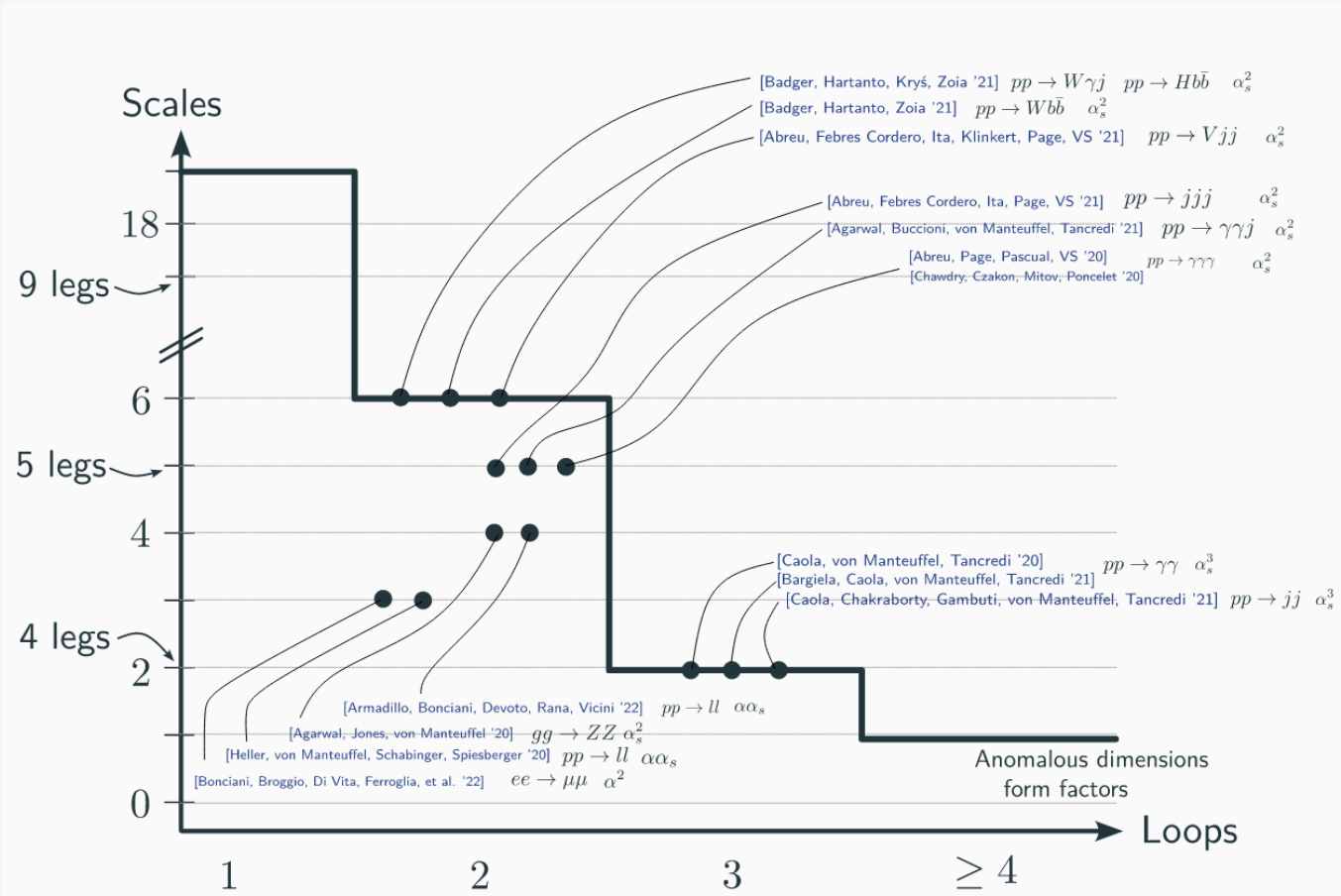

Warning: a biased selection of references!

Still not automated, systematic, even at 2nd order, though the progress in methods and tools impressive

just one example

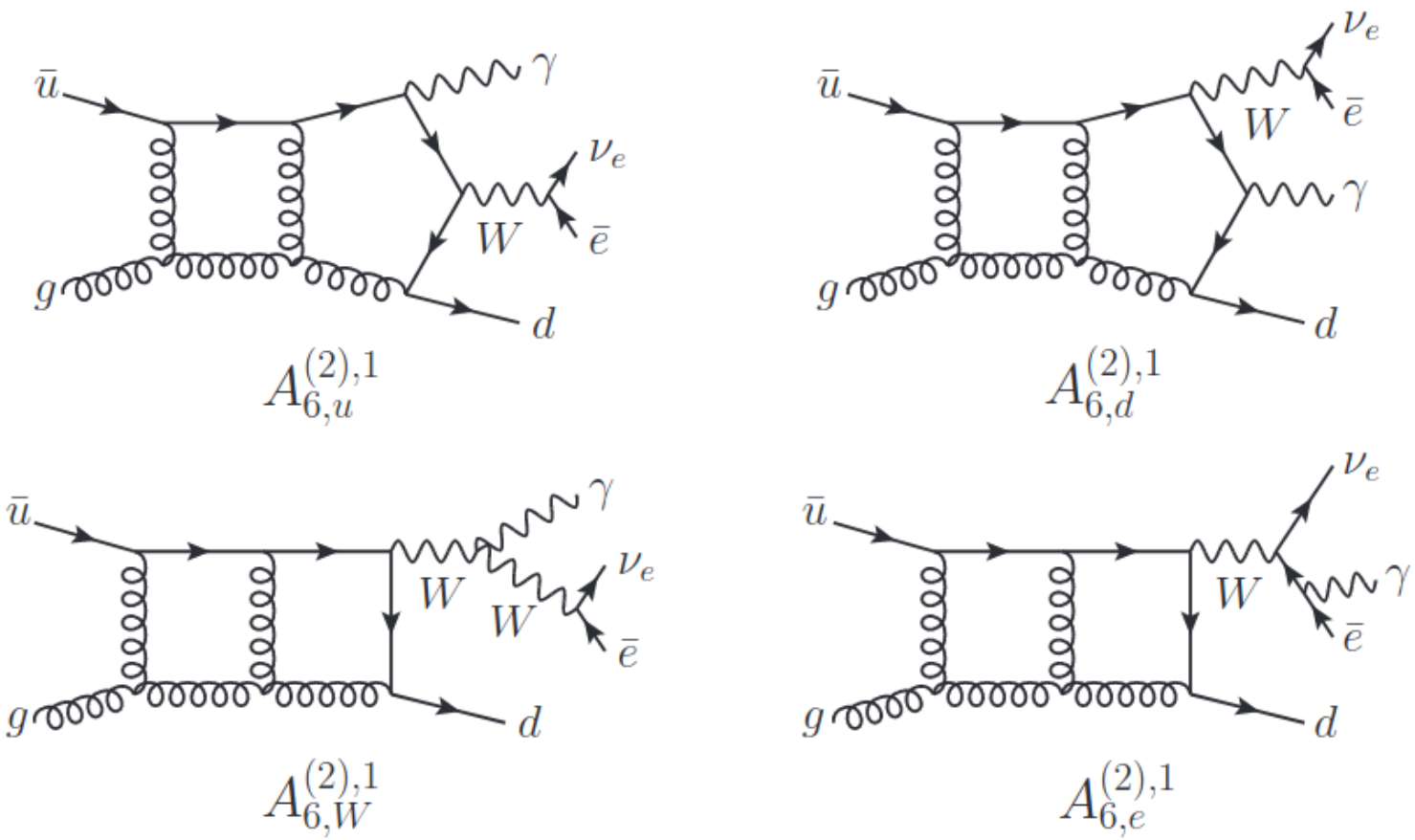

Figure 1. Sample two-loop Feynman diagrams for $W^+\gamma j$ production.

Łamanie symetrii i kształt potencjału

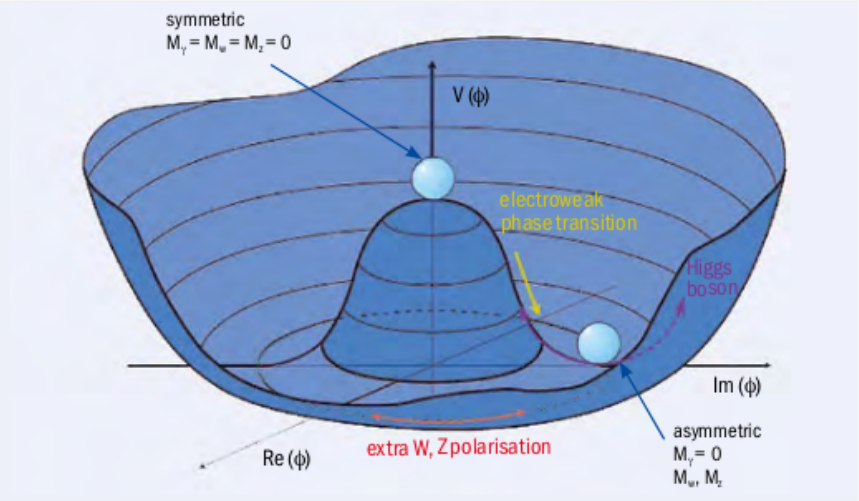

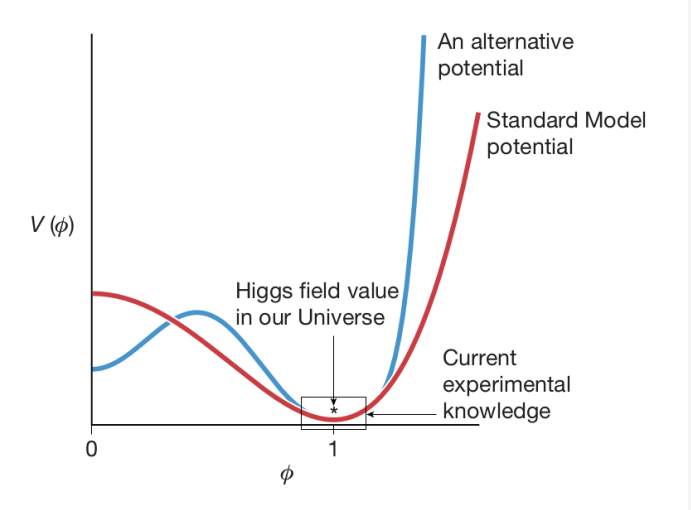

$$\Phi \equiv \Phi_{SM} = \begin{pmatrix} \phi^+ \\ \phi^0 \end{pmatrix}$$

$$V = -\mu^2 \Phi^\dagger \Phi + \lambda (\Phi^\dagger \Phi)^2 \Leftrightarrow y = ax + bx^2, y \equiv V, x \equiv \Phi^\dagger \Phi$$

$$V_{min} = v/\sqrt{2}, v = \sqrt{\mu^2/\lambda} \simeq 250 \text{ GeV}$$

Łamanie symetrii i kształt potencjału, konsekwencje

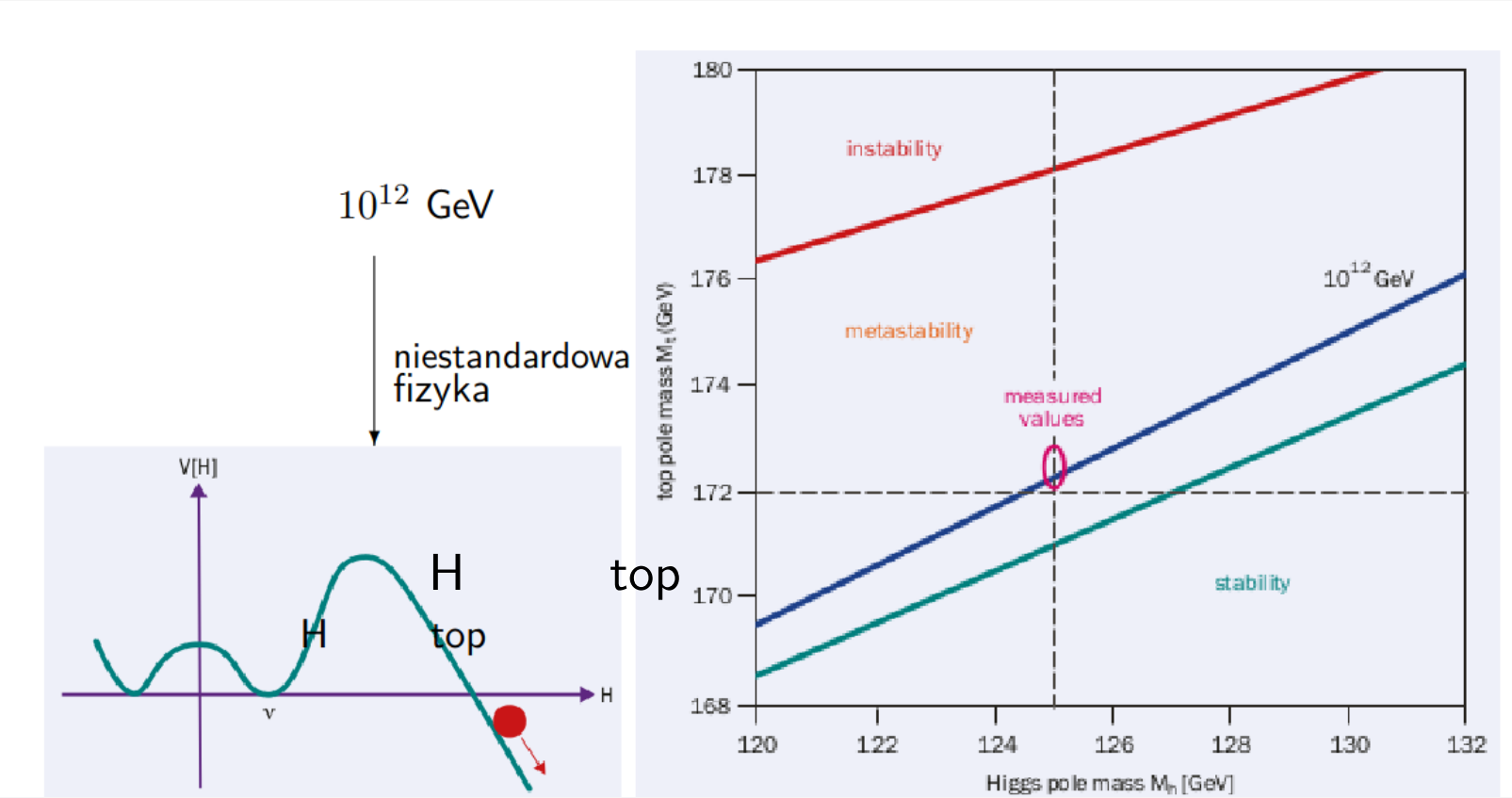

Jorgen D'Hondt, "Strategies and plans for particle physics in Europe",

Epiphany 2021, https://indico.cern.ch/event/934666

---

e^+e^- Higgs Factories

circular colliders

4y @ M_Z (150ab^{-1})
1-2y @ 2xM_W (10ab^{-1})
3y @ 240 GeV (5ab^{-1})
5y @ 2xm_t (1.5ab^{-1})

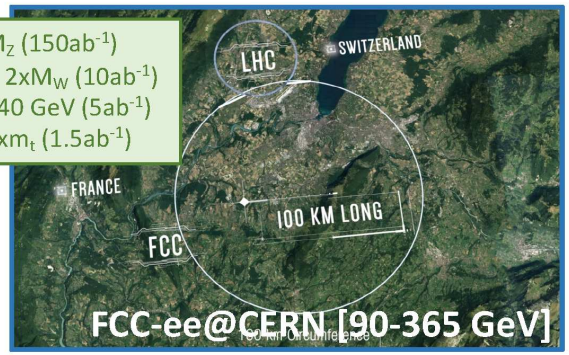

FCC-ee@CERN [90-365 GeV]

CEPC@China [90-240-(350) GeV]

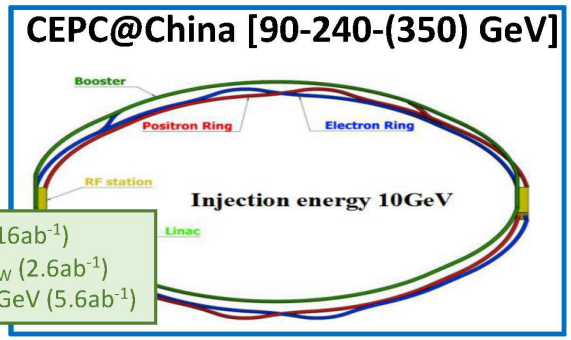

2y @ M_Z (16ab^{-1})
1y @ 2xM_W (2.6ab^{-1})
7y @ 240 GeV (5.6ab^{-1})

linear colliders

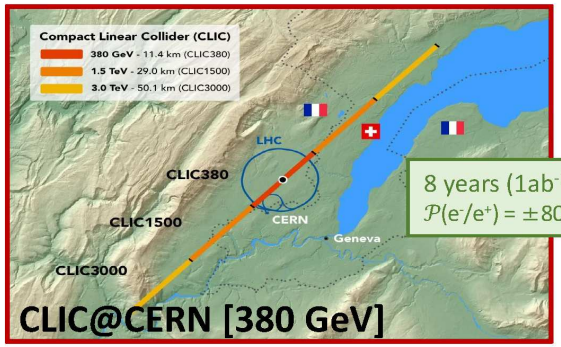

CLIC@CERN [380 GeV]

8 years (1ab^{-1})
$\mathcal{P}(e^-/e^+) = \pm 80\%/0\%$

ILC@Japan [250 GeV]

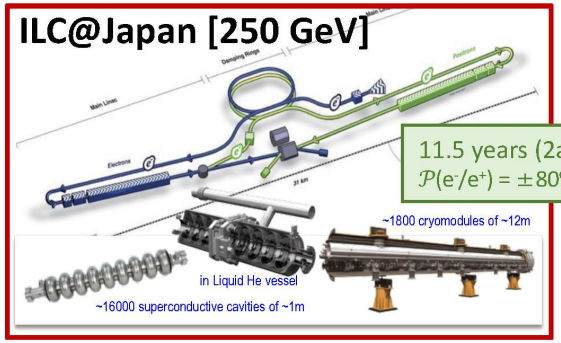

11.5 years (2ab^{-1})
$\mathcal{P}(e^-/e^+) = \pm 80\%/\pm 30\%$

Jorgen D'Hondt, "Strategies and plans for particle physics in Europe",

Epiphany 2021, https://indico.cern.ch/event/934666

---

e^+e^- Higgs Factories (incl. B/c/τ/EW/top factories)

precision frontier — circular colliders

synchrotron radiation

for the same power, less luminosity at higher E_{cm}

(Energy Recovery Linac technology might mitigate this & allow to go to higher E_{cm})

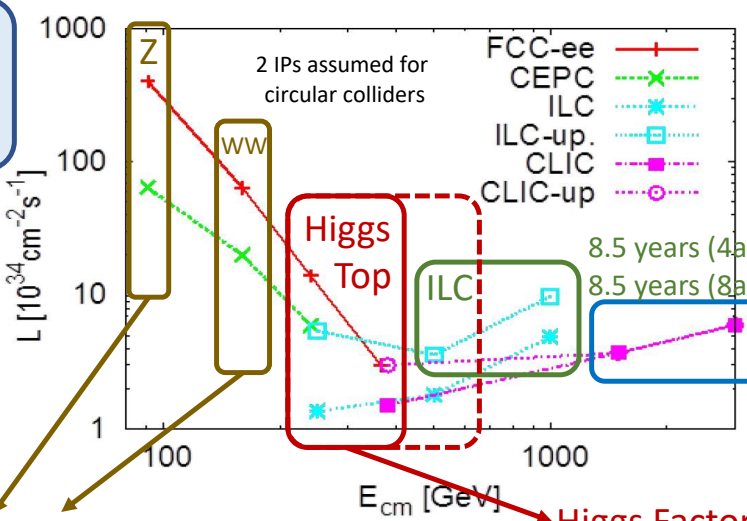

linear colliders — energy frontier

8.5 years (4ab^{-1} @ 0.5 TeV)
8.5 years (8ab^{-1} @ 1 TeV)
7 years (2.5ab^{-1} @ 1.5 TeV)
8 years (5ab^{-1} @ 3 TeV)

B/c/τ/EW Factories

per detector in e^+e^-	# Z	# B	# τ	# charm	# WW
LEP	4×10^6	1×10^6	3×10^5	1×10^6	2×10^4
SuperKEKB	-	10^{11}	10^{11}	10^{11}	-
FCC-ee	2.5×10^{12}	7.5×10^{11}	2×10^{11}	6×10^{11}	1.5×10^8

Higgs Factories with complementarity

- g_{HZZ} (250GeV) versus g_{HWW} (380GeV)
- top quark physics
- beam polarization for EW precision tests

(transverse polarization in circular e^+e^- colliders only at lower E_{cm} while longitudinal polarization at linear colliders)

25

Czy pomiar α ma wpływ na niestandardowe modele (BSM)?

Table 1 | Error budget on α

Source	Correction ($\times 10^{-13}$)	Relative uncertainty ($\times 10^{-13}$)
Gravity gradient	−0.6	0.1
Alignment of the beams	0.5	0.5
Coriolis acceleration		1.2
Frequencies of the lasers		0.3
Wave-front curvature	0.6	0.3
Wave-front distortion	3.9	1.9
Gouy phase	108.2	5.4
Residual Raman light shift	2.3	2.3
Index of refraction	0	<0.1
Internal interaction	0	<0.1
Light shift (two-photon transition)	−11.0	2.3
Second-order Zeeman effect		0.1
Phase shifts in Raman phase-lock loop	−39.8	0.6
Global systematic effects	**64.2**	**6.8**
Statistical uncertainty		**2.4**
Relative mass of ^{87}Rb[a]: 86.9091805310(60)		3.5
Relative mass of the electron[b]: 5.48579909065(16) × 10^{-4}		1.5
Rydberg constant[b]: 10,973,731.568160(21) m^{-1}		0.1
Total: α^{-1} = 137.035999206(11)		**8.1**

For each systematic effect, more discussion can be found in Methods.
[a]From ref. [13].
[b]From https://pml.nist.gov/cuu/Constants/.

Morel, L., Yao, Z., Cladé, P. et al. Determination of the fine-structure constant with an accuracy of 81 parts per trillion. Nature 588, 61–65 (2020).

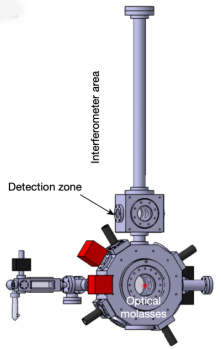

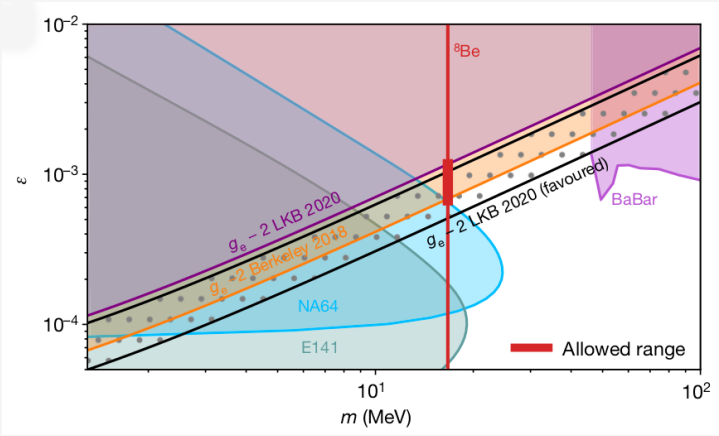

Podstruktura: m^*, rozmiar $L = \hbar/(m^* c) \longrightarrow$ dodatkowa modyfikacja rzędu $\delta a_e \simeq m_e/m^*$
stąd wykluczone:

$$m^* < 520 \text{ GeV} \equiv L > 2 \times 10^{-18}/4 \times 10^{-19} \text{ m}$$

Eksperyment ma polepszyć dokładność δa_e o rząd w następnych latach, będzie na poziomie czułości $(g-2)_\mu$.

Ograniczenia

U wielomian dla nieplanarnego 3-pętlowego pudełka (64 człony)

```
x[1] x[2] x[4] + x[1] x[3] x[4] + x[2] x[3] x[4] + x[1] x[2] x[5] +
x[1] x[3] x[5] + x[2] x[3] x[5] + x[1] x[4] x[5] + x[2] x[4] x[5] +
x[2] x[4] x[6] + x[3] x[4] x[6] + x[2] x[5] x[6] + x[3] x[5] x[6] +
x[4] x[5] x[6] + x[2] x[4] x[7] + x[3] x[4] x[7] + x[2] x[5] x[7] +
x[3] x[5] x[7] + x[4] x[5] x[7] + x[1] x[2] x[8] + x[1] x[3] x[8] +
x[2] x[3] x[8] + x[1] x[4] x[8] + x[2] x[4] x[8] + x[2] x[6] x[8] +
x[3] x[6] x[8] + x[4] x[6] x[8] + x[2] x[7] x[8] + x[3] x[7] x[8] +
x[4] x[7] x[8] + x[1] x[2] x[9] + x[1] x[3] x[9] + x[2] x[3] x[9] +
x[2] x[4] x[9] + x[3] x[4] x[9] + x[1] x[5] x[9] + x[3] x[5] x[9] +
x[4] x[5] x[9] + x[2] x[6] x[9] + x[3] x[6] x[9] + x[5] x[6] x[9] +
x[2] x[7] x[9] + x[3] x[7] x[9] + x[5] x[7] x[9] + x[1] x[8] x[9] +
x[3] x[8] x[9] + x[4] x[8] x[9] + x[6] x[8] x[9] + x[7] x[8] x[9] +
x[1] x[2] x[10] + x[1] x[3] x[10] + x[2] x[3] x[10] +
x[1] x[4] x[10] + x[2] x[4] x[10] + x[2] x[6] x[10] +
x[3] x[6] x[10] + x[4] x[6] x[10] + x[2] x[7] x[10] +
x[3] x[7] x[10] + x[4] x[7] x[10] + x[1] x[9] x[10] +
x[3] x[9] x[10] + x[4] x[9] x[10] + x[6] x[9] x[10] + x[7] x[9] x[10]
```

F-wielomian Symanzika: problem $\Gamma[0]$, twierdzenie Cheng-Wu

- 2-loop: $\delta(1-v_1-v_2)$, $U(\vec{v}) = v_3 + v_1 v_2$
  brak dodatkowych całek MB from U
- 3-loop: $\delta(1-v_1-v_2-v_3)$
  - "ladder" - 2 dodatkowe całki MB 64-dim $\rightarrow$ 2-dim (!)
  - "mercedes" - 4 dodatowe całki MB

Aby otrzymać minimalny wymiar:

- 1-loop: $U(\vec{x}) \equiv 1$ gdziekolwiek możliwe
- 2- i 3-pętle: wyrażenie dla F nie rozwijane

$$F = F_0 + U \sum_{i=1}^{N} x_i m_i^2$$

Drugi człon można rozszerzyć (generujac progi, bez potrzeby deformacji konturu) lub nie (mniejsza wymiarowość kosztem gorszej zintegrowanej zbieżności)

Metoda AMFlow, $\eta = \infty \longrightarrow \eta = 0^+$

analityczna kontynuacja (pływ dodatkowej masy)

---

2. Prace Jan 27 2022 papers by Zhi-Feng Liu, Yan-Qin Ma and Xiao Liu: https://inspirehep.net/literature/2020677, https://inspirehep.net/literature/2020676, https://inspirehep.net/literature/2020880 and 1711.09572 https://inspirehep.net/literature/1639025.

$$\begin{aligned}
\widetilde{I}_{\vec{\nu}}(\eta) &= \int \left(\prod_{i=1}^{L} \frac{\mathrm{d}^D \ell_i}{i\pi^{D/2}} \right) \frac{\widetilde{\mathcal{D}}_{K+1}^{-\nu_{K+1}} \cdots \widetilde{\mathcal{D}}_{N}^{-\nu_N}}{\widetilde{\mathcal{D}}_{1}^{\nu_1} \cdots \widetilde{\mathcal{D}}_{K}^{\nu_K}}. \\
\widetilde{\mathcal{D}}_1 &= \ell_1^2 - m^2 + \mathrm{i}\eta \\
I_{\vec{\nu}} &= \lim_{\eta \to 0^+} \widetilde{I}_{\vec{\nu}}(\eta) \\
\mathrm{i}\frac{\partial}{\partial \eta} \vec{\widetilde{J}}(\eta) &= A(\eta) \widetilde{J}(\eta)
\end{aligned}$$

Key point: warunki brzegowe przy $\eta \to \infty$ są ca␣lkami pęcherzykowymi (bubbles) pojedynczej skali masy, rozwiązywanymi iteracyjnie .

MIs dużej dokładności z AMFlow, wyniki

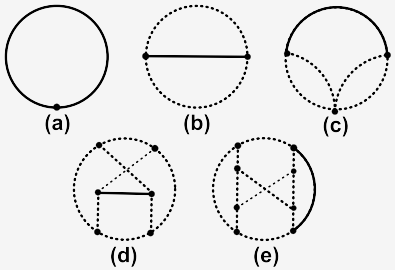

$$I_{\vec{\nu}} = \int \left(\prod_{i=1}^{L} \frac{{}^{D}\ell_i}{\pi^{D/2}} \right) \frac{\mathcal{D}_{K+1}^{-\nu_{K+1}} \cdots \mathcal{D}_{N}^{-\nu_N}}{\mathcal{D}_1^{\nu_1} \cdots \mathcal{D}_K^{\nu_K}}, \quad \mathcal{D}_1 = \ell_1^2 - m^2 + 0^+$$

$$\widehat{I}_{\vec{\nu}'}(\ell_1^2) = \int \left(\prod_{i=2}^{L} \frac{{}^{D}\ell_i}{\pi^{D/2}} \right) \frac{\mathcal{D}_{K+1}^{-\nu_{K+1}} \cdots \mathcal{D}_{N}^{-\nu_N}}{\mathcal{D}_2^{\nu_2} \cdots \mathcal{D}_K^{\nu_K}}, \quad I_{\vec{\nu}} = \{\Gamma[\ldots]\}\widehat{I}_{\vec{\nu}'}(-m^2)$$

L-**loop** $(L\text{-}1)$-**loop**

$$\begin{aligned} I[(e)] = &- 2.073855510286740\epsilon^{-2} - 7.812755312590133\epsilon^{-1} \\ &- 17.25882864945875 + 717.6808845492140\epsilon \\ &+ 8190.876448160049\epsilon^2 + 78840.29598046500\epsilon^3 \\ &+ 566649.1116484678\epsilon^4 + 3901713.802716081\epsilon^5 \\ &+ 23702384.71086095\epsilon^6 + 14214293.68205112\epsilon^7, \end{aligned}$$

10 orders in ϵ, 16-digit precision.
Such an exact boundary point can be transported by `DiffExp` to any physical point.